

Massive Spin-1 Field Chiral Lagrangian from an Extended Nambu–Jona-Lasinio Model of QCD

Joaquim Prades

Centre de Physique Théorique, C.N.R.S. - Luminy, Case 907
F-13288 Marseille Cedex 9, France

Abstract

We present a calculation of the coupling constants in the massive spin-1 field chiral Lagrangian to chiral $\mathcal{O}(p^3)$ in the context of the extended Nambu–Jona-Lasinio model described in Ref. [1]. Phenomenological applications of this Lagrangian to anomalous and non-anomalous low-energy hadronic transitions involving spin-1 particles are also discussed.

1 Introduction

At low-energies the strong, electromagnetic and weak interactions of the lightest pseudoscalar mesons can be described by an effective chiral Lagrangian [2, 3]. This Lagrangian depends on a number of coupling constants which are not fixed by symmetry requirements alone but are, in principle, determined by the dynamics of the underlying QCD theory. Recently, there have been attempts to derive the low-energy effective chiral action of QCD [1, 4] with and without the inclusion of the low-lying resonances. The lightest vector, axial-vector and scalar resonances play an important rôle in the determination of the low-energy interactions between pseudoscalar mesons in the context of chiral Lagrangians at $\mathcal{O}(p^4)$ as shown in Ref. [5].

In this work we shall study the chiral Lagrangians for spin-1 particles to $\mathcal{O}(p^3)$ in the chiral expansion, in the context of the extended Nambu–Jona-Lasinio (ENJL) cut-off model described in Ref. [1]. In particular, we shall calculate the couplings of spin-1 particles to Goldstone bosons and external sources. As an application, we shall then predict the decay rates for the transitions $V \rightarrow \pi\gamma$, $V \rightarrow \pi\pi\pi$, $V \rightarrow \pi\pi\gamma$, $V \rightarrow V'\gamma$, $V \rightarrow V'\pi$, $A \rightarrow \pi\pi\pi$, $A \rightarrow \pi\gamma$, $A \rightarrow V\pi$ and $A \rightarrow V\gamma$. Here V and A denote vector and axial-vector particles. We shall also discuss the vector meson dominance predictions for the $\pi^0 \rightarrow \gamma\gamma^*$ and $K_L \rightarrow \pi^0\gamma^*\gamma^* \rightarrow \pi^0 e^+e^-$ transitions. The paper is organized as follows. In Section 2 we give a brief summary of what is known about low-energy chiral Lagrangians from general symmetry requirements alone. In Section 3 we summarize some of the ENJL results found in Ref. [1]. In Section 4 we shall then study the anomalous sector of the theory and in Section 5 the non-anomalous sector. Finally, in Section 6 we discuss the phenomenological applications to the decays involving spin-1 particles. The conclusions are given in Section 7.

2 The low-energy chiral Lagrangians

We shall give a summary of what is known at present about low-energy mesonic Lagrangians, from the chiral invariance properties of \mathcal{L}_{QCD} alone. In the pseudoscalar sector, the terms in the effective Lagrangian \mathcal{L}_{eff} with the lowest chiral dimension, *i.e.* $\mathcal{O}(p^2)$, are

$$\mathcal{L}_{\text{eff}}^{(2)} = \frac{1}{4} f_0^2 \left\{ \text{tr} \left(D_\mu U D^\mu U^\dagger \right) + \text{tr} \left(\chi U^\dagger + U \chi^\dagger \right) \right\} \quad (2.1)$$

where D_μ denotes the covariant derivative

$$D_\mu U = \partial_\mu U - i(v_\mu + a_\mu)U + iU(v_\mu - a_\mu), \quad (2.2)$$

and $U \equiv \exp\left(-\frac{\sqrt{2}i\Phi}{f_0}\right)$ an SU(3) matrix incorporating the octet of pseudoscalar mesons

$$\Phi(x) = \frac{\vec{\lambda}}{\sqrt{2}} \vec{\varphi} = \begin{pmatrix} \frac{\pi^0}{\sqrt{2}} + \frac{\eta_8}{\sqrt{6}} & \pi^+ & K^+ \\ \pi^- & -\frac{\pi^0}{\sqrt{2}} + \frac{\eta_8}{\sqrt{6}} & K^0 \\ K^- & \bar{K}^0 & -\frac{2\eta_8}{\sqrt{6}} \end{pmatrix}. \quad (2.3)$$

In Eq. (2.2) v_μ, a_μ are external 3×3 vector and axial-vector field matrices. In Eq. (2.1)

$$\chi = 2B_0(s(x) + ip(x)), \quad (2.4)$$

with s and p external scalar and pseudoscalar 3×3 field matrices. In practice

$$\chi = 2B_0\mathcal{M} \quad (2.5)$$

with \mathcal{M} the 3×3 flavour matrix $\mathcal{M} = \text{diag}(m_u, m_d, m_s)$ which collects the light-quark masses. The constants f_0 and B_0 are not fixed by chiral symmetry requirements. The constant f_0 can be obtained from $\pi \rightarrow \mu\nu$ decay [6],

$$f_0 \simeq f_\pi \simeq 93 \text{ MeV}. \quad (2.6)$$

The constant B_0 is related to the vacuum expectation value

$$\langle 0|\bar{q}q|0\rangle_{|q=u,d,s} = -f_0^2 B_0(1 + \mathcal{O}(\mathcal{M})). \quad (2.7)$$

In the absence of the $U(1)_A$ anomaly, the SU(3) singlet η_1 field becomes the ninth Goldstone boson which is incorporated in the $\Phi(x)$ field as

$$\Phi(x) = \frac{\vec{\lambda}}{\sqrt{2}} \vec{\varphi} + \frac{\eta_1}{\sqrt{3}} \mathbf{1}. \quad (2.8)$$

The terms in \mathcal{L}_{eff} of $\mathcal{O}(p^4)$ are also known. They have been discussed extensively by Gasser and Leutwyler [3].

We are interested in an effective Lagrangian $\mathcal{L}_{\text{eff}}^R$ which also incorporates chiral couplings of fields of massive 1^- , 1^+ and 0^+ states to the Goldstone fields. We shall restrict ourselves to the sector of spin-1 particles. The general method to construct these couplings was described a long time ago in Ref. [7]. An explicit construction can be found in Refs. [5] and [8]. As discussed in Ref. [8], the choice of fields to describe chiral invariant couplings involving spin-1 particles is not unique and, when the vector modes are integrated out, leads to ambiguities in the context of chiral perturbation theory to $\mathcal{O}(p^4)$ and higher. As shown in [8], these ambiguities are, however, removed when consistency with the short-distance behaviour of QCD is incorporated. The effective Lagrangian which we shall choose here to describe spin-1 particle couplings corresponds to the so-called model II in Ref. [8]. In this model the linear couplings of vector and axial-vector fields to the pseudoscalar mesons and external fields start at chiral $\mathcal{O}(p^3)$. The most general Lagrangian $\mathcal{L}_{\text{eff}}^R$ for spin-1 particles to lowest non-trivial order in the chiral expansion and linear in the spin-1 fields for the interaction terms is then obtained by adding to $\mathcal{L}_{\text{eff}}^{(2)}$ in Eq. (2.1) the vector Lagrangian

$$\begin{aligned}
\mathcal{L}_V = & -\frac{1}{4} \text{tr} (V_{\mu\nu} V^{\mu\nu} - 2 M_V^2 V_\mu V^\mu) \\
& -\frac{1}{2\sqrt{2}} \left[f_V \text{tr} (V_{\mu\nu} f_{(+)}^{\mu\nu}) + i g_V \text{tr} (V_{\mu\nu} [\xi^\mu, \xi^\nu]) \right] \\
& + i \alpha_V \text{tr} (V_\mu [\xi_\nu, f_{(-)}^{\mu\nu}]) + \beta_V \text{tr} (V_\mu [\xi^\mu, \chi_{(-)}]) + i \theta_V \epsilon_{\mu\nu\alpha\beta} \text{tr} (V^\mu \xi^\nu \xi^\alpha \xi^\beta) \\
& + h_V \epsilon_{\mu\nu\alpha\beta} \text{tr} (V^\mu \{ \xi^\nu, f_{(+)}^{\alpha\beta} \}) ,
\end{aligned} \tag{2.9}$$

and the axial-vector Lagrangian

$$\begin{aligned}
\mathcal{L}_A = & -\frac{1}{4} \text{tr} (A_{\mu\nu} A^{\mu\nu} - 2 M_A^2 A_\mu A^\mu) - \frac{1}{2\sqrt{2}} f_A \text{tr} (A_{\mu\nu} f_{(-)}^{\mu\nu}) \\
& + i \alpha_A \text{tr} (A_\mu [\xi_\nu, f_{(+)}^{\mu\nu}]) + \gamma_A^{(1)} \text{tr} (A_\mu \xi_\nu \xi^\mu \xi^\nu) + \gamma_A^{(2)} \text{tr} (A_\mu \{ \xi^\mu, \xi^\nu \xi_\nu \}) \\
& + \gamma_A^{(3)} \text{tr} (A_\mu \xi_\nu) \text{tr} (\xi^\mu \xi^\nu) + \gamma_A^{(4)} \text{tr} (A_\mu \xi^\mu) \text{tr} (\xi^\nu \xi_\nu) \\
& + h_A \epsilon_{\mu\nu\alpha\beta} \text{tr} (A^\mu \{ \xi^\nu, f_{(-)}^{\alpha\beta} \}) .
\end{aligned} \tag{2.10}$$

The notation here is the following. We assume nonet symmetry for the spin-1 particles, so that the spin-1 fields we consider are

$$\begin{aligned}
V^\mu &= V_8^\mu + V_1^\mu \\
A^\mu &= A_8^\mu + A_1^\mu
\end{aligned} \tag{2.11}$$

where V_8^μ and A_8^μ are $SU(3)_V$ octets while V_1^μ and A_1^μ are singlets. The vector field matrix $V_8^\mu(x)$:

$$V_8^\mu(x) \equiv \begin{pmatrix} \frac{\rho^0}{\sqrt{2}} + \frac{\omega_8}{\sqrt{6}} & \rho^+ & K^{*+} \\ \rho^- & -\frac{\rho^0}{\sqrt{2}} + \frac{\omega_8}{\sqrt{6}} & K^{*0} \\ K^{*-} & \frac{K^{*0}}{K^{*0}} & -\frac{2\omega_8}{\sqrt{6}} \end{pmatrix}^\mu, \tag{2.12}$$

represents the $SU(3)_V$ octet of spin-parity 1^- -particles and the axial-vector field matrix $A_8^\mu(x)$:

$$A_8^\mu(x) \equiv \begin{pmatrix} \frac{a_1^0}{\sqrt{2}} + \frac{(f_1)_8}{\sqrt{6}} & a_1^+ & K_1^+ \\ a_1^- & -\frac{a_1^0}{\sqrt{2}} + \frac{(f_1)_8}{\sqrt{6}} & K_1^0 \\ K_1^- & \frac{K_1^0}{K_1^0} & -\frac{2(f_1)_8}{\sqrt{6}} \end{pmatrix}^\mu, \tag{2.13}$$

represents the $SU(3)_V$ octet of spin-parity 1^+ -particles. The vector field matrix $V_1(x)$:

$$V_1(x) \equiv \frac{\omega_1}{\sqrt{3}} \mathbf{1}, \tag{2.14}$$

represents the $SU(3)_V$ singlet of spin-parity 1^- -particles and the axial-vector field matrix $A_1(x)$ represents the corresponding $SU(3)_V$ singlet of spin-parity 1^+ -particles. The vector and axial-vector field strength tensors are defined as follows

$$V_{\mu\nu} = d_\mu V_\nu - d_\nu V_\mu \quad \text{and} \quad A_{\mu\nu} = d_\mu A_\nu - d_\nu A_\mu. \tag{2.15}$$

Here, the covariant derivative d_μ acts on the octet multiplets denoted by R_8 as follows

$$d_\mu R_8 = \partial_\mu R_8 + [\Gamma_\mu, R_8] \quad (2.16)$$

and trivially on the singlets. The connection Γ_μ is given by

$$\Gamma_\mu = \frac{1}{2} \left\{ \xi^\dagger [\partial_\mu - i(v_\mu + a_\mu)] \xi + \xi [\partial_\mu - i(v_\mu - a_\mu)] \xi^\dagger \right\}. \quad (2.17)$$

The axial-vector field matrix ξ_μ is defined by

$$\xi_\mu = i \left\{ \xi^\dagger [\partial_\mu - i(v_\mu + a_\mu)] \xi - \xi [\partial_\mu - i(v_\mu - a_\mu)] \xi^\dagger \right\} = i \xi^\dagger D_\mu U \xi^\dagger = \xi_\mu^\dagger. \quad (2.18)$$

Finally, in Eqs. (2.9) and (2.10), we have also introduced the following objects

$$\chi_{(\pm)} = \xi^\dagger \chi \xi^\dagger \pm \xi \chi^\dagger \xi, \quad (2.19)$$

and

$$f_{(\pm)}^{\mu\nu} = \xi F_L^{\mu\nu} \xi^\dagger \pm \xi^\dagger F_R^{\mu\nu} \xi, \quad (2.20)$$

with $F_L^{\mu\nu}$ and $F_R^{\mu\nu}$ the external field-strength tensors

$$F_L^{\mu\nu} = \partial^\mu l^\nu - \partial^\nu l^\mu - i [l^\mu, l^\nu], \quad (2.21)$$

$$F_R^{\mu\nu} = \partial^\mu r^\nu - \partial^\nu r^\mu - i [r^\mu, r^\nu] \quad (2.22)$$

associated with the external left (l_μ) and right (r_μ) field sources

$$l_\mu = v_\mu - a_\mu, \quad r_\mu = v_\mu + a_\mu. \quad (2.23)$$

In this paper, we are also interested in couplings of vector and axial-vector quadratic in the spin-1 fields. The complete set of these quadratic interaction terms for vector meson fields, to lowest chiral $\mathcal{O}(p^2)$, is

$$\begin{aligned}
\mathcal{L}_{VV}^{(2)} = & \frac{1}{2} \delta_V^{(1)} \text{tr}([\xi_\mu, \xi_\nu][V^\mu, V^\nu]) + \frac{1}{2} \delta_V^{(2)} \text{tr}([V_\mu, \xi_\nu][V^\nu, \xi^\mu]) \\
& + \frac{1}{2} \delta_V^{(3)} \text{tr}([V_\mu, \xi^\mu][V_\nu, \xi^\nu]) + \frac{1}{2} \delta_V^{(4)} \text{tr}(V^\mu V^\nu \xi_\mu \xi_\nu) + \frac{1}{2} \delta_V^{(5)} \text{tr}(V^\mu V_\mu \xi^\nu \xi_\nu) \\
& + \frac{1}{2} \delta_V^{(6)} \text{tr}(V^\mu \xi^\nu V_\mu \xi_\nu) + \frac{1}{2} i \phi_V \text{tr}\left(V_\mu [V_\nu, f_{(+)}^{\mu\nu}]\right) \\
& + \frac{1}{2} \sigma_V \epsilon_{\mu\nu\alpha\beta} \text{tr}\left(V^\mu \{\xi^\nu, V^{\alpha\beta}\}\right).
\end{aligned} \tag{2.24}$$

The corresponding interaction terms for axial-vector meson fields are

$$\begin{aligned}
\mathcal{L}_{AA}^{(2)} = & \frac{1}{2} \delta_A^{(1)} \text{tr}([\xi_\mu, \xi_\nu][A^\mu, A^\nu]) + \frac{1}{2} \delta_A^{(2)} \text{tr}([A_\mu, \xi_\nu][A^\nu, \xi^\mu]) \\
& + \frac{1}{2} \delta_A^{(3)} \text{tr}([A_\mu, \xi^\mu][A_\nu, \xi^\nu]) + \frac{1}{2} \delta_A^{(4)} \text{tr}(A^\mu A^\nu \xi_\mu \xi_\nu) + \frac{1}{2} \delta_A^{(5)} \text{tr}(A^\mu A_\mu \xi^\nu \xi_\nu) \\
& + \frac{1}{2} \delta_A^{(6)} \text{tr}(A^\mu \xi^\nu A_\mu \xi_\nu) + \frac{1}{2} i \phi_A \text{tr}\left(A_\mu [A_\nu, f_{(+)}^{\mu\nu}]\right) \\
& + \frac{1}{2} \sigma_A \epsilon_{\mu\nu\alpha\beta} \text{tr}\left(A^\mu \{\xi^\nu, A^{\alpha\beta}\}\right).
\end{aligned} \tag{2.25}$$

At $\mathcal{O}(p^2)$ there are also terms which mix axial-vector and vector fields. The corresponding interaction Lagrangian has the following form,

$$\begin{aligned}
\mathcal{L}_{VA}^{(2)} = & i A^{(1)} \text{tr}\left(V_\mu [A_\nu, f_{(-)}^{\mu\nu}]\right) + i A^{(2)} \text{tr}(V_\mu [\xi_\nu, A^{\mu\nu}]) + i A^{(3)} \text{tr}(A_\mu [\xi_\nu, V^{\mu\nu}]) \\
& + B \text{tr}\left(V_\mu [A^\mu, \chi_{(-)}]\right) + H \epsilon_{\mu\nu\alpha\beta} \text{tr}\left(V^\mu \{A^\nu, f_{(+)}^{\alpha\beta}\}\right) \\
& + i Z^{(1)} \epsilon_{\mu\nu\alpha\beta} \text{tr}\left(\xi^\mu \xi^\nu \{A^\alpha, V^\beta\}\right) + i Z^{(2)} \epsilon_{\mu\nu\alpha\beta} \text{tr}\left(\xi^\mu A^\nu \xi^\alpha V^\beta\right).
\end{aligned} \tag{2.26}$$

In the present work we shall concentrate on processes involving spin-1 particles and we shall not consider possible spin-1 particle decays to scalar particles. Whenever scalar particles can contribute as intermediate resonances to these transitions, in particular for a_1 -decays, we cannot integrate them out since their masses are lower than those of the axial-vector particles and they have to be taken into account as propagating particles described by the corresponding Lagrangian. The effective Lagrangian for scalar particles that may contribute to the transitions we are interested

in is of chiral $\mathcal{O}(p^2)$. To this order, the most general Lagrangian for 0^+ -particles involving at most one scalar and two spin-1 fields is

$$\begin{aligned} \mathcal{L}_S = & \frac{1}{2} \text{tr} (d_\mu S d^\mu S - M_S^2 S^2) + c_m \text{tr} (S \chi^+) + c_d \text{tr} (S \xi^\mu \xi_\mu) \\ & + C^{(1)} \text{tr} (S \{A_\mu, \xi^\mu\}) + \frac{1}{2} C^{(2)} \text{tr} (S A^\mu A_\mu) + \frac{1}{2} D \text{tr} (S V^\mu V_\mu) . \end{aligned} \quad (2.27)$$

Here, the 3×3 field matrix S represents the $\text{SU}(3)_V$ nonet of scalar fields. The chiral $\mathcal{O}(p^2)$ couplings c_m and c_d in the ENJL cut-off model have been calculated in Ref. [1].

3 The ENJL cut-off model of QCD

Reference [1] gives a systematic study of the low-energy effective action of the extended Nambu–Jona-Lasinio model which, at intermediate energies below or of the order of a cut-off scale Λ_χ , is expected to be a good effective realization of the standard QCD Lagrangian \mathcal{L}_{QCD} . Here we give a brief summary of the results found there. The Lagrangian in question is

$$\begin{aligned} \mathcal{L}_{\text{QCD}} \rightarrow & \mathcal{L}_{\text{QCD}}^{\Lambda_\chi} + \mathcal{L}_{\text{NJL}}^{\text{S,P}} + \mathcal{L}_{\text{NJL}}^{\text{V,A}} + \mathcal{O} \left(\frac{1}{\Lambda_\chi^4} \right) , \\ \text{with } \mathcal{L}_{\text{NJL}}^{\text{S,P}} = & \frac{8\pi^2 G_S(\Lambda_\chi)}{N_c \Lambda_\chi^2} \sum_{i,j} (\bar{q}_R^i q_L^j) (\bar{q}_L^j q_R^i) \end{aligned} \quad (3.1)$$

and

$$\mathcal{L}_{\text{NJL}}^{\text{V,A}} = - \frac{8\pi^2 G_V(\Lambda_\chi)}{N_c \Lambda_\chi^2} \sum_{i,j} \left[(\bar{q}_L^i \gamma^\mu q_L^j) (\bar{q}_L^j \gamma_\mu q_L^i) + (L \rightarrow R) \right] .$$

Where i, j are flavour indices and $\Psi_R^L \equiv \frac{1}{2} (1 \pm \gamma_5) \Psi$. The couplings G_S and G_V are dimensionless and $\mathcal{O}(1)$ in the $1/N_c$ -expansion. In the mean-field approximation, these $\mathcal{L}_{\text{NJL}}^{\text{S,P,V,A}}$ above are equivalent to the constituent chiral quark-mass term [4]:

$$- M_Q (\bar{q}_R U q_L + \bar{q}_L U^\dagger q_R) . \quad (3.2)$$

In the presence of this term it is useful to introduce new quark fields Q_L and Q_R , which we call “rotated basis”, or constituent, chiral-quarks [9], defined as follows

$$\begin{aligned}
Q_L &= \xi q_L; & \bar{Q}_L &= \bar{q}_L \xi^\dagger; \\
Q_R &= \xi^\dagger q_R; & \bar{Q}_R &= \bar{q}_R \xi.
\end{aligned}
\tag{3.3}$$

In the rest of this Section we shall work in Euclidean space for convenience, and we shall adopt the conventions given in Ref. [1]. The effective action, in the presence of external sources l_μ and r_μ and light-quark-mass matrix \mathcal{M} , can be written as [1]

$$\begin{aligned}
e^{\Gamma_{\text{eff}}(H, \xi, W_\mu^\pm; l_\mu, r_\mu, \mathcal{M})} &= \\
&\exp \left(- \int d^4x \left\{ \frac{N_c \Lambda_\chi^2}{8\pi^2 G_S(\Lambda_\chi)} \text{tr} H^2 + \frac{N_c \Lambda_\chi^2}{64\pi^2 G_V(\Lambda_\chi)} \text{tr} (W_\mu^+ W_\mu^+ + W_\mu^- W_\mu^-) \right\} \right) \\
&\quad \times \frac{1}{Z} \int [\mathcal{D} G_\mu] \exp \Gamma_E(\mathcal{A}_\mu, M),
\end{aligned}
\tag{3.4}$$

where $W_\mu^\pm(x)$ and $H(x)$ are 3×3 auxiliary Hermitian field matrices which under the chiral group transform as

$$\begin{aligned}
W_\mu^\pm &\rightarrow h(\Phi, g_{L,R}) W_\mu^\pm h^\dagger(\Phi, g_{L,R}), \\
H &\rightarrow h(\Phi, g_{L,R}) H h^\dagger(\Phi, g_{L,R}),
\end{aligned}
\tag{3.5}$$

where $h(\Phi, g_{L,R}) \equiv h$ is the compensating $\text{SU}(3)_V$ transformation which appears under the action of the chiral group $G \equiv \text{SU}(3)_L \times \text{SU}(3)_R$ on the coset representative $\xi(\Phi)$ of the $G/\text{SU}(3)_V$ manifold, *i.e.*

$$\xi(\Phi) \rightarrow g_R \xi(\Phi) h^\dagger = h \xi(\Phi) g_L^\dagger,
\tag{3.6}$$

where $\xi(\Phi)\xi(\Phi) = U$ in the chosen gauge. In the mean-field approximation these field matrices are replaced by

$$\begin{aligned}
H &\Rightarrow M_Q \mathbf{1}, \\
W_\mu^\pm &\Rightarrow 0.
\end{aligned}
\tag{3.7}$$

In Eq. (3.4) we have used the short-hand notation

$$[\mathcal{D} G_\mu] \equiv \mathcal{D} G_\mu \exp \left(- \frac{1}{4} \sum_{a=1}^{N_c^2-1} G_{\rho\nu}^{(a)} G_{\rho\nu}^{(a)} \right)
\tag{3.8}$$

with $G_{\mu\nu}^{(a)}$ the gluon field strength tensor and

$$\exp \Gamma_E(\mathcal{A}_\mu, M) = \int \mathcal{D}\bar{Q} \mathcal{D}Q \exp \int d^4x \bar{Q} D_E Q = \det D_E \quad (3.9)$$

where D_E is the Euclidean Dirac operator

$$D_E = \gamma_\mu \nabla_\mu + M = \gamma_\mu (\partial_\mu + \mathcal{A}_\mu) + M \quad (3.10)$$

with

$$\begin{aligned} \mathcal{A}_\mu &= i G_\mu + \Gamma_\mu - \frac{i}{2} \gamma_5 (\xi_\mu - W_\mu^-) - \frac{i}{2} W_\mu^+; \\ M &= -H - \frac{1}{2} (\Sigma - \gamma_5 \Delta) \end{aligned} \quad (3.11)$$

and

$$\begin{aligned} \Sigma &= \xi^\dagger \mathcal{M} \xi^\dagger + \xi \mathcal{M}^\dagger \xi; \\ \Delta &= \xi^\dagger \mathcal{M} \xi^\dagger - \xi \mathcal{M}^\dagger \xi. \end{aligned} \quad (3.12)$$

In Eq. (3.11) G_μ is the gluon field matrix in the fundamental $SU(N_c)$ representation and the connection Γ_μ and axial-vector field ξ_μ are given in Eqs. (2.17) and (2.18). In our calculation of the fermionic determinant we shall disregard the gluonic corrections due to fluctuations below the cut-off scale Λ_χ and shall consider a model that is more like the first alternative envisaged in Ref. [1], where the formal integration over gluon fields has been done in the path-integral of the generating functional for Green functions. Our choice here is motivated by the fact that the results obtained within this alternative in Ref. [1] for the couplings of the low-energy chiral Lagrangian to $\mathcal{O}(p^4)$ are not qualitatively different from those obtained in the same Reference when the effect of long-distance gluonic interactions was taken into account.

In Ref. [1] it was pointed out that the effective action in Eq. (3.4) obeys the following formal symmetry: the effective action $\Gamma_E(\mathcal{A}_\mu, M)$ with \mathcal{A}_μ and M given in Eq. (3.11) can be written formally as the mean-field approximation expression corresponding to external sources l_μ and r_μ and light-quark-mass matrix \mathcal{M} redefined as follows,

$$\begin{aligned}
l_\mu &\rightarrow l'_\mu = l_\mu + \frac{1}{2} \xi^\dagger (W_\mu^+ + W_\mu^-) \xi, \\
r_\mu &\rightarrow r'_\mu = r_\mu + \frac{1}{2} \xi (W_\mu^+ - W_\mu^-) \xi^\dagger, \\
\mathcal{M} &\rightarrow \mathcal{M}' = \mathcal{M} + \xi \sigma \xi.
\end{aligned} \tag{3.13}$$

Here,

$$\sigma \equiv H - M_Q \mathbf{1} \tag{3.14}$$

is a 0^+ -field matrix. We shall use this formal symmetry in the following Sections.

Once the quarks and gluons in the effective action in Eq. (3.4) are integrated out (see Ref. [1]), one can get the correct kinetic term for spin-1 particles after two steps. The first one is the diagonalization of the quadratic form in ξ_μ and $W_\mu^{(-)}$ that defines the constant g_A , *i.e.*

$$W_\mu^{(-)} \rightarrow \widehat{W}_\mu^{(-)} + (1 - g_A) \xi_\mu. \tag{3.15}$$

The second one is a scale redefinition of the fields $W_\mu^{(+)}$ and $\widehat{W}_\mu^{(-)}$, *i.e.*

$$V_\mu = \frac{f_V}{\sqrt{2}} W_\mu^{(+)}, \quad A_\mu = \frac{f_A}{g_A \sqrt{2}} \widehat{W}_\mu^{(-)} \tag{3.16}$$

that introduces the physical vector and axial-vector fields V_μ and A_μ . All the couplings of the low-energy effective action can then be obtained as functions of three parameters only, g_A , M_Q and Λ_χ . The $\mathcal{O}(p^3)$ couplings f_V , g_V and f_A have been already calculated in Ref. [1] with the results to leading $\mathcal{O}(N_c)$,

$$\begin{aligned}
f_V^2 &= \frac{N_c}{16\pi^2} \frac{2}{3} \Gamma(0, x), & f_A^2 &= \frac{N_c}{16\pi^2} \frac{2g_A^2}{3} [\Gamma(0, x) - \Gamma(1, x)], \\
g_V &= \frac{N_c}{16\pi^2} \frac{1}{3f_V} [(1 - g_A^2) \Gamma(0, x) + 2g_A^2 \Gamma(1, x)].
\end{aligned} \tag{3.17}$$

Here,

$$x = \frac{M_Q^2}{\Lambda_\chi^2} \tag{3.18}$$

and the function $\Gamma(n, x)$ is the incomplete Gamma function

$$\Gamma(n, x) = \int_x^\infty \frac{dz}{z} e^{-z} z^n, \quad n = 0, 1, \dots \quad (3.19)$$

The correct kinetic term for 0^+ -particles is obtained after a scale redefinition of the σ field in Eq. (3.13), *i.e.*

$$S = \lambda_S \sigma \quad (3.20)$$

that introduces the physical 0^+ -field S . The constant λ_S was calculated in this model in Ref. [1],

$$\lambda_S^2 = \frac{N_c}{16\pi^2} \frac{2}{3} [3\Gamma(0, x) - 2\Gamma(1, x)]. \quad (3.21)$$

In the present work we want to calculate the rest of the $\mathcal{O}(p^3)$ couplings in the Lagrangians in Eqs. (2.9), (2.10) and (2.27) as well as the $\mathcal{O}(p^2)$ couplings of the interaction Lagrangians in Eqs. (2.24), (2.25) and (2.26). We shall later study some of the phenomenological applications of our results. We first consider the terms that carry a Levi-Civita pseudotensor, *i.e.* the abnormal intrinsic parity terms [10].

4 The anomalous sector

Here we are concerned with the imaginary part of the effective action. The lowest order Lagrangian in the abnormal intrinsic parity sector describing the interaction of pseudoscalar mesons and external l_μ and r_μ sources is the one given by the Wess-Zumino (WZ) effective action [11, 12]. The $\mathcal{O}(p^6)$ imaginary part of the effective action has been obtained in Ref. [10] in the mean-field approximation of the model we consider here. Using the formal symmetry in the ENJL cut-off model described above in Section 3, we can obtain to $\mathcal{O}(p^3)$ the abnormal intrinsic parity interaction terms for spin-1 particles from an effective action that formally has the same expression as that of the WZ action but with the external sources l_μ and r_μ replaced by the primed sources in Eq. (3.13).

The WZ effective action [11, 12] has the following explicit form in a scheme where vector currents are conserved:

$$\begin{aligned}
S_{WZ}[U, l, r] = & -\frac{i N_c}{240\pi^2} \int d\sigma^{ijklm} \text{tr} \left(\Sigma_i^L \Sigma_j^L \Sigma_k^L \Sigma_l^L \Sigma_m^L \right) \\
& -\frac{i N_c}{48\pi^2} \int d^4x \epsilon_{\mu\nu\alpha\beta} \left(W(U, l, r)^{\mu\nu\alpha\beta} - W(\mathbf{1}, l, r)^{\mu\nu\alpha\beta} \right), \tag{4.1}
\end{aligned}$$

where

$$\begin{aligned}
W(U, l, r)_{\mu\nu\alpha\beta} = & \text{tr} \left(U l_\mu l_\nu l_\alpha U^\dagger r_\beta + \frac{1}{4} U l_\mu U^\dagger r_\nu U l_\alpha U^\dagger r_\beta + i U \partial_\mu l_\nu l_\alpha U^\dagger r_\beta \right. \\
& + i \partial_\mu r_\nu U l_\alpha U^\dagger r_\beta - i \Sigma_\mu^L l_\nu U^\dagger r_\alpha U l_\beta + \Sigma_\mu^L U^\dagger \partial_\nu r_\alpha U l_\beta \\
& - \Sigma_\mu^L \Sigma_\nu^L U^\dagger r_\alpha U l_\beta + \Sigma_\mu^L l_\nu \partial_\alpha l_\beta + \Sigma_\mu^L \partial_\nu l_\alpha l_\beta \\
& \left. - i \Sigma_\mu^L l_\nu l_\alpha l_\beta + \frac{1}{2} \Sigma_\mu^L l_\nu \Sigma_\alpha^L l_\beta - i \Sigma_\mu^L \Sigma_\nu^L \Sigma_\alpha^L l_\beta \right) \\
& - (L \leftrightarrow R)
\end{aligned}$$

$$\text{with} \quad \Sigma_\mu^L = U^\dagger \partial_\mu U, \quad \Sigma_\mu^R = U \partial_\mu U^\dagger \quad \text{and} \quad \epsilon_{0123} = 1. \tag{4.2}$$

Here, $(L \leftrightarrow R)$ stands for the interchanges

$$U \leftrightarrow U^\dagger, \quad l_\mu \leftrightarrow r_\mu, \quad \Sigma_\mu^L \leftrightarrow \Sigma_\mu^R. \tag{4.3}$$

The first term in Eq. (4.1) is an integration of an antisymmetric $SU(3)_L \times SU(3)_R$ invariant fifth-rank tensor that does not contain external sources over a five-dimensional sphere whose boundary is four-dimensional Minkowski space [12].

We can now show how the formal symmetry of the ENJL cut-off version of QCD explained in Section 3 works. As an example we are going to calculate the term that is modulated by the coupling constant h_V in Eq. (2.9). We can write down the interaction Lagrangian linear in the $W_\mu^{(+)}$ field as

$$\mathcal{L}_I^{W^{(+)}} \equiv \text{tr} \left(W_\mu^{(+)} J^\mu \right). \tag{4.4}$$

To obtain the current J^μ , first we calculate the left (L_μ) and right (R_μ) anomalous chiral currents from the WZ effective action above, *i.e.*

$$\begin{aligned}
\tilde{L}^\mu &\equiv \frac{\delta S_{WZ}}{\delta l_\mu} \equiv L^\mu + \text{non-chirally covariant polynomial} \\
&\quad \text{in external sources,} \\
\tilde{R}^\mu &\equiv \frac{\delta S_{WZ}}{\delta r_\mu} \equiv R^\mu + \text{non-chirally covariant polynomial} \\
&\quad \text{in external sources.}
\end{aligned} \tag{4.5}$$

The anomalous currents \tilde{L}^μ and \tilde{R}^μ have the well known structure [13, 14] which consists of a chirally covariant part (L^μ and R^μ) that is scheme independent and a non-chirally covariant polynomial in external sources that depends on the scheme. Of course, the physics is contained in the chirally covariant part and does not change with the scheme. It is then easy to see that the current J^μ we want in Eq. (4.4) can be obtained as follows,

$$J^\mu = \frac{1}{2} \left[\xi L^\mu \xi^\dagger + \xi^\dagger R^\mu \xi \right] \left| \begin{array}{l} l_\mu \rightarrow l_\mu + \frac{1}{2} \xi^\dagger W_\mu^{(-)} \xi \\ r_\mu \rightarrow r_\mu - \frac{1}{2} \xi W_\mu^{(-)} \xi^\dagger \end{array} \right. . \tag{4.6}$$

The result we get for the term we are interested in is

$$\mathcal{L}_I^{W^{(+)}} \doteq \frac{N_c}{48\pi^2} \frac{1}{4} \epsilon^{\mu\nu\alpha\beta} \text{tr} \left(W_\mu^{(+)} \left\{ 3\xi_\nu - 2W_\nu^{(-)}, f_{\alpha\beta}^{(+)} \right\} \right). \tag{4.7}$$

As was explained in Section 3, to obtain the interaction Lagrangian of the physical vector field V_μ from $\mathcal{L}_I^{W^{(+)}}$ we have to perform the shift in Eq. (3.15) and the scale redefinition in Eq. (3.16). These two operations introduce the couplings g_A , f_V and f_A which collect the information of the underlying theory that has been integrated out. The Lagrangian that we obtain then for the term we are considering is

$$\mathcal{L}_I^V \doteq \frac{N_c}{16\pi^2} \frac{\sqrt{2}}{4f_V} \left(1 - \frac{2}{3}(1 - g_A) \right) \epsilon^{\mu\nu\alpha\beta} \text{tr} \left(V_\mu \left\{ \xi_\nu, f_{\alpha\beta}^{(+)} \right\} \right). \tag{4.8}$$

After performing the same kind of calculations as in the example above, for the other abnormal intrinsic parity terms in Eqs. (2.9), (2.10), (2.24), (2.25) and (2.26) we get the following results for these couplings:

$$\begin{aligned}
\theta_V &= \frac{N_c}{16\pi^2} \frac{\sqrt{2}}{3f_V} \left(1 + \frac{(1+g_A)(1-g_A^2)}{8} \right), & h_V &= \frac{N_c}{16\pi^2} \frac{\sqrt{2}}{4f_V} \left(1 - \frac{2}{3}(1-g_A) \right), \\
h_A &= \frac{N_c}{16\pi^2} \frac{g_A^2 \sqrt{2}}{12f_A}, & \sigma_V &= \frac{N_c}{16\pi^2} \frac{1}{2f_V^2} \left(1 - \frac{2}{3}(1-g_A) \right), \\
\sigma_A &= \frac{N_c}{16\pi^2} \frac{g_A^2}{6f_A^2}, & H &= -\frac{N_c}{16\pi^2} \frac{g_A}{6f_A f_V}, \\
Z^{(1)} &= -\frac{N_c}{16\pi^2} \frac{g_A(5+4g_A-g_A^2)}{12f_A f_V}, & Z^{(2)} &= -\frac{N_c}{16\pi^2} \frac{g_A(1+g_A)^2}{12f_A f_V}.
\end{aligned} \tag{4.9}$$

We therefore find that these couplings, in the ENJL model we are considering, are completely fixed by the constants f_V , f_A and g_A . This is due to the fact that the terms in the abnormal intrinsic parity sector for the interaction of spin-1 fields with pseudoscalar mesons and external sources to chiral $\mathcal{O}(p^3)$ and the WZ effective action come from the same formal expression.

From the expressions in Eq. (4.9), we find relations between the various couplings that are independent of g_A ,

$$\begin{aligned}
\frac{h_V}{\sigma_V} &= \frac{f_V}{\sqrt{2}} \\
\frac{h_A}{\sigma_A} &= \frac{f_A}{\sqrt{2}}.
\end{aligned} \tag{4.10}$$

These relations appear because of the formal symmetry between the expression for the mean-field approximation effective action and the effective action including spin-1 particle fields explained in Section 3. Because of that symmetry we have, for instance, that in the effective action $f_{\mu\nu}^{(+)}$ and $V_{\mu\nu}$ always appear in the following combination

$$f_{\mu\nu}^{(+)} + \frac{\sqrt{2}}{f_V} V_{\mu\nu}, \tag{4.11}$$

therefore the couplings σ_V and h_V are related as given in Eq. (4.10).

The abnormal intrinsic parity couplings involving spin-1 particles have been considered in the literature in the context of different models [15]-[18]. A common feature of these models which differentiates them from the ENJL cut-off model we are studying here is that the spin-1 particles are introduced there as the gauge bosons either of a hidden local symmetry [15, 16] or of the $U(3)_L \times U(3)_R$ chiral symmetry

[17]. The derivation of the models in Refs. [15]-[17] from an ENJL model in the presence of the chiral anomaly is studied in Ref. [19]. In this Reference, special attention is given to the equivalence of these models for the physics in the anomalous and non-anomalous sectors of the theory. The most interesting of these models is the so-called Hidden Gauge Symmetry (HGS) model [15, 16]. In this model, vector mesons are the dynamical gauge bosons of a hidden local $U(3)_V$ symmetry of the chiral Lagrangian. Ref. [16] gives the general solution for the chiral anomaly in the presence of vector mesons when considered as gauge bosons. The solution is a linear combination of six invariants which, in general, introduce interaction terms between Goldstone bosons and external sources apart from those contained in the WZ action. It was also shown there that these new interaction terms do not change the low-energy theorems for $\pi^0 \rightarrow \gamma\gamma$ and $\gamma \rightarrow \pi\pi\pi$ transitions. The ENJL model we consider here does not introduce any coupling between Goldstone bosons and external sources apart from those in the WZ action. Thus, in order to compare both models, we shall require that the linear combination of six invariants which is a solution of the anomaly in the HGS model does not introduce couplings between Goldstone bosons and external sources apart from those in the WZ action. In this limit we have that the following relation, already found in the ENJL model in Eq. (4.10),

$$\frac{h_V}{\sigma_V} = \frac{f_V}{\sqrt{2}} \quad (4.12)$$

is also present in the HGS model. In the same limit one also finds the following relation in the HGS model

$$\frac{\theta_V}{h_V} = 2, \quad (4.13)$$

which in the ENJL model is only true for a particular value of the g_A coupling. This value is a solution of the following equation,

$$5 - 7g_A - g_A^2 - g_A^3 = 0 \quad (4.14)$$

and is $g_A \simeq 0.63$. (The other two solutions are not real.)

5 The non-anomalous sector

We shall next study the real part of the effective action, *i.e.* the non-anomalous sector of the theory. This sector can be computed in the ENJL cut-off theory proposed in Ref. [1], as was shown there, with the help of the heat kernel expansion

[20]. We shall use the formal symmetry stated in Section 3 as we did in the anomalous sector in Section 4. Therefore to obtain the effective action in terms of the spin-1 fields $W_\mu^{(\pm)}$ we only need to calculate the effective action in the mean-field approximation limit and replace the external sources by the primed external sources in Eq. (3.13). (For a summary of the main technical details and notation see Ref. [1].) As explained in Section 3, from this effective action we can get the effective action involving the physical spin-1 particle fields V_μ and A_μ by performing the diagonalization and scale redefinition in Eqs. (3.15) and (3.16).

Within this approach we calculate the non-anomalous couplings of spin-1 particles to pseudoscalar mesons and external sources at leading $\mathcal{O}(N_c)$ for terms that are linear or quadratic in the spin-1 particle fields and to chiral $\mathcal{O}(p^3)$. The results for the couplings in the Lagrangian in Eq. (2.9) are

$$\begin{aligned}\alpha_V &= -\frac{N_c}{16\pi^2} \frac{\sqrt{2}g_A^2}{6f_V} [\Gamma(0, x) - \Gamma(1, x)] , \\ \beta_V &= -\frac{N_c}{16\pi^2} \frac{\sqrt{2}g_A}{12f_V} [3\rho\Gamma(0, x) + \Gamma(1, x)] \\ &\text{with } \rho \equiv \frac{M_Q}{B_0} .\end{aligned}\tag{5.1}$$

For the couplings in the Lagrangian in Eq. (2.10) we get

$$\begin{aligned}\alpha_A &= -\frac{N_c}{16\pi^2} \frac{\sqrt{2}g_A^2}{6f_A} [\Gamma(0, x) - 2\Gamma(1, x)] , \\ \gamma_A^{(1)} &= \frac{N_c}{16\pi^2} \frac{\sqrt{2}g_A^2}{6f_A} [(1 - g_A^2)\Gamma(0, x) \\ &\quad - 2(1 - 2g_A^2)\Gamma(1, x) - 2g_A^2\Gamma(2, x)] , \\ \gamma_A^{(2)} &= -\frac{N_c}{16\pi^2} \frac{\sqrt{2}g_A^2}{12f_A} [(1 - g_A^2)\Gamma(0, x) \\ &\quad - 2(1 - 4g_A^2)\Gamma(1, x) - 4g_A^2\Gamma(2, x)] , \\ \gamma_A^{(3)} &= \mathcal{O}(1/\sqrt{N_c}) \quad \text{and} \quad \gamma_A^{(4)} = \mathcal{O}(1/\sqrt{N_c}) .\end{aligned}\tag{5.2}$$

For the couplings in the Lagrangian in Eq. (2.24) we get

$$\begin{aligned}
\delta_V^{(1)} &= -\frac{N_c}{16\pi^2} \frac{1}{12f_V^2} [(2 - 3g_A^2)\Gamma(0, x) + 7g_A^2\Gamma(1, x)] , \\
-4\delta_V^{(2)} &= -4\delta_V^{(3)} = -\delta_V^{(5)} = \\
\delta_V^{(6)} &= \frac{N_c}{16\pi^2} \frac{g_A^2}{3f_V^2} [\Gamma(0, x) - \Gamma(1, x)] , \\
\delta_V^{(4)} &= \mathcal{O}(1/N_c) , \\
\phi_V &= \frac{N_c}{16\pi^2} \frac{1}{3f_V^2} [\Gamma(0, x) - \Gamma(1, x)] .
\end{aligned} \tag{5.3}$$

For the couplings in the Lagrangian in Eq. (2.25) we get

$$\begin{aligned}
\delta_A^{(1)} &= -\frac{N_c}{16\pi^2} \frac{g_A^2}{12f_A^2} [(2 - 3g_A^2)\Gamma(0, x) \\
&\quad - 4(1 - 6g_A^2)\Gamma(1, x) - 12g_A^2\Gamma(2, x)] , \\
\delta_A^{(2)} &= \delta_A^{(3)} = -\frac{N_c}{16\pi^2} \frac{g_A^4}{12f_A^2} [\Gamma(0, x) - 8\Gamma(1, x) - 4\Gamma(2, x)] , \\
\delta_A^{(4)} &= \mathcal{O}(1/N_c) , \\
\delta_A^{(5)} &= -\frac{N_c}{16\pi^2} \frac{g_A^4}{3f_A^2} [\Gamma(0, x) - 8\Gamma(1, x) + 4\Gamma(2, x)] , \\
\delta_A^{(6)} &= \frac{N_c}{16\pi^2} \frac{g_A^4}{3f_A^2} [\Gamma(0, x) - 4\Gamma(1, x) + 2\Gamma(2, x)] , \\
\phi_A &= \frac{N_c}{16\pi^2} \frac{g_A^2}{3f_A^2} \Gamma(0, x) .
\end{aligned} \tag{5.4}$$

For the couplings in the Lagrangian in Eq. (2.26) we get

$$\begin{aligned}
A^{(1)} &= A^{(2)} = -\frac{N_c}{16\pi^2} \frac{g_A^2}{3f_A f_V} [\Gamma(0, x) - \Gamma(1, x)] , \\
A^{(3)} &= -\frac{N_c}{16\pi^2} \frac{g_A^2}{3f_A f_V} [\Gamma(0, x) - 2\Gamma(1, x)] , \\
B &= -\frac{N_c}{16\pi^2} \frac{g_A}{2f_A f_V} \rho \Gamma(0, x) .
\end{aligned} \tag{5.5}$$

Finally, for the couplings in the Lagrangian in Eq. (2.27) we get

$$\begin{aligned}
C^{(1)} &= -\frac{\sqrt{2}}{f_A} c_d, & C^{(2)} &= \frac{4}{f_A^2} c_d \\
\text{with} \quad c_d &= \frac{N_c}{16\pi^2} \frac{M_Q}{\lambda_S} 2 g_A^2 [\Gamma(0, x) - \Gamma(1, x)], \\
D &= 0.
\end{aligned} \tag{5.6}$$

From the expressions in Eqs. (5.1)-(5.6) we can obtain the following relations that are independent of g_A ,

$$\begin{aligned}
\frac{\alpha_V}{A^{(1)}} &= \frac{\alpha_V}{A^{(2)}} = \frac{f_A}{\sqrt{2}} \\
\frac{\alpha_A}{A^{(3)}} &= \frac{f_V}{\sqrt{2}} \\
\frac{C^{(1)}}{C^{(2)}} &= -\frac{f_A}{2\sqrt{2}}
\end{aligned} \tag{5.7}$$

which are also due to the formal symmetry explained in Section 3, like the relations in Eq. (4.10).

6 Phenomenological applications

In this Section we shall discuss some phenomenological applications from our calculations. In the whole following analysis we shall work in the chiral limit, *i.e.* $\mathcal{M} \rightarrow 0$. Therefore, we shall disregard possible $\omega_8 - \rho^0$ and $\eta_8 - \pi^0$ mixings, which are proportional to light-quark masses. In addition, the operators that generate these mixings are order $\mathcal{O}(p^4)$ in the chiral expansion [21]. Here we shall use the coupling constants we have calculated in the previous Sections in the ENJL cut-off model [1] to make predictions on a large variety of processes where spin-1 particle are involved (anomalous transitions, radiative decays, \dots). The radiative decays of vector mesons in the context of Zweig's rule and explicit SU(3)-symmetry violation induced by a non-vanishing strange-quark mass was considered in Ref. [22] in the non-relativistic quark model. The different coupling constants appearing there were fixed from a fit to experimental data. Phenomenology involving spin-1 particles has been discussed before within different approaches. See for instance Refs. [22]- [27].

6.1 Vector resonance decays

Here we shall discuss the predictions for vector particle decays. As was already mentioned in Section 3, in the ENJL model we are considering, all the couplings can

be written in terms of three parameters, namely g_A , M_Q and Λ_χ . The coupling g_A was defined in Eq. (3.15) and in this model takes the following value [1]

$$g_A = 1 - \frac{f_\pi^2}{f_V^2 M_V^2}. \quad (6.1)$$

We shall choose for g_A , M_Q and Λ_χ the values that are obtained from fitting the $\mathcal{O}(p^2)$ and $\mathcal{O}(p^4)$ couplings of the chiral Lagrangian [1], *i.e.*

$$g_A = 0.65, \quad x \equiv \frac{M_Q^2}{\Lambda_\chi^2} = 0.06 \quad \text{and} \quad M_Q = 260 \text{ MeV}. \quad (6.2)$$

These values correspond to $f_V = 0.17$, $g_V = 0.083$ and $f_A = 0.080$.

For the vector mixing $\omega - \phi$ we use the ideal angle, *i.e.* $\tan \varphi_V = 1/\sqrt{2}$ and for the pseudoscalar mixing we use $\tan \varphi_P = -1/2\sqrt{2}$. In both cases we assume nonet symmetry. The diagonalized ω , ϕ , η and η' states in terms of the SU(3) octet and singlet states in Eqs. (2.3), (2.8), (2.12) and (2.14) are

$$\begin{aligned} \eta' &= \cos \varphi_P \eta_1 + \sin \varphi_P \eta_8, \\ \eta &= -\sin \varphi_P \eta_1 + \cos \varphi_P \eta_8, \\ \omega &= \cos \varphi_V \omega_1 + \sin \varphi_V \omega_8, \\ \phi &= -\sin \varphi_V \omega_1 + \cos \varphi_V \omega_8. \end{aligned} \quad (6.3)$$

First we shall study the decays $V \rightarrow P\gamma$ ($P \rightarrow V\gamma$), for which the Feynman diagrams are shown in Figure 1. The amplitude for the $V \rightarrow P\gamma$ decay is given by the expression

$$\begin{aligned} A(V \rightarrow P(p)\gamma(k)) &= C_{VP\gamma} 4 |e| \sqrt{2} \frac{h_V}{f_\pi} \epsilon_{\mu\nu\alpha\beta} \varepsilon_{(\gamma)}^\mu k^\nu \varepsilon_{(V)}^{*\alpha} p^\beta \\ &\times \left[1 + \sqrt{2} \frac{f_V \sigma_V}{h_V} \frac{k^2}{M_{V'}^2 - k^2 - i M_{V'} \Gamma_{V'}} \right]. \end{aligned} \quad (6.4)$$

Here, $C_{VP\gamma}$ is an SU(3)-light-flavour symmetry factor that relates the different amplitudes. The different values for this factor and the intermediate resonance V' appearing in Eq. (6.4) for each process are given in Table 1. We denote the polarization pseudovector corresponding to the particle V by $\varepsilon_{(V)}^\mu$. The decay rate corresponding to the amplitude in Eq. (6.4) is

$$\Gamma(V \rightarrow P\gamma) = |C_{VP\gamma}|^2 \frac{4\alpha h_V^2 M_V^3}{3 f_\pi^2} \lambda^{3/2} \left(1, \frac{m_P^2}{M_V^2}, \frac{k^2}{M_V^2} \right) \times \left| 1 + \frac{2k^2}{M_{V'}^2 - k^2 - i M_{V'} \Gamma_{V'}} \right|^2, \quad (6.5)$$

with $\alpha = \frac{e^2}{4\pi}$ and

$$\lambda(x, y, z) = x^2 + y^2 + z^2 - 2xy - 2xz - 2yz. \quad (6.6)$$

Table 1: SU(3)-symmetry factors ($C_{VP\gamma}$) and intermediate resonance (V') for the $V \rightarrow P\gamma$ ($P \rightarrow V\gamma$) decays.

Process	$C_{VP\gamma}$	V'
$\rho \rightarrow \pi\gamma$	1/3	ω_8
$\omega \rightarrow \pi^0\gamma$	1	ρ^0
$\rho^0 \rightarrow \eta\gamma$	$-\sqrt{2}/\sqrt{3}$	ρ^0
$\omega \rightarrow \eta\gamma$	$\sqrt{2}/(3\sqrt{3})$	ω_8
$\eta' \rightarrow \rho^0\gamma$	1	ρ^0
$\eta' \rightarrow \omega\gamma$	1/3	ω_8
$\phi \rightarrow \pi^0\gamma$	0	ρ^0
$\phi \rightarrow \eta\gamma$	$2/(3\sqrt{3})$	ω_8
$\phi \rightarrow \eta'\gamma$	$-2\sqrt{2}/\sqrt{3}$	ω_8
$K^{*0} \rightarrow K^0\gamma$	2/3	—
$K^{*+} \rightarrow K^+\gamma$	1/3	—

The decay rates for the ω and ρ^0 vectors can have contributions from a possible $\omega_8 - \rho^0$ mixing. In addition, the amplitude for $\rho \rightarrow \pi\gamma$ has a sizable contribution from the absorptive part of pion and kaon chiral loops (see Figure 2). (For the other processes this contribution is negligible.) We have taken into account this last contribution which has the following expression

$$\Gamma(\rho \rightarrow \pi\gamma)|_{\text{Abs}} = \frac{\alpha g_V^2 M_\rho^{11}}{(768\sqrt{6})^2 \pi^6 f_\pi^{10}} \left(1 - \frac{m_\pi^2}{M_\rho^2} \right)^3 \left(1 - \frac{4m_\pi^2}{M_\rho^2} \right)^3. \quad (6.7)$$

The predictions listed in the column Prediction 1 in Table 2 correspond to the values of g_A , M_Q and x in Eq. (6.2). The worst results in this column, taking into account the experimental errors, are for the decays $\phi \rightarrow \eta\gamma$ and $K^{*+} \rightarrow K^+\gamma$ which are between 4 and 6 standard deviations (σ) from the experimental value. These disintegrations, however, can be explained with the inclusion of explicit chiral symmetry breaking terms proportional to the strange-quark mass as shown in the non-relativistic quark model in Ref. [22]. The predictions for the other processes are less than 2 σ from the central experimental values. The processes $\rho^0 \rightarrow \pi^0\gamma$ and $\omega \rightarrow \pi^0\gamma$ are likely to be influenced by a possible $\omega_8 - \rho^0$ mixing. All the predictions for the transitions in Table 2 are made in the chiral limit and depend on two couplings, h_V and g_V ; in fact the constant g_V only affects to $\rho \rightarrow \pi\gamma$ decays and its contribution is not dominant. We refrain from doing a fit of the experimental results since all the amplitudes are related by SU(3)-symmetry factors (up to the small part proportional to g_V in $\rho \rightarrow \pi\gamma$ decays) and higher order chiral corrections for these processes are very different for each of them.

Table 2: Partial widths in keV corresponding to $V \rightarrow P\gamma$ and $P \rightarrow V\gamma$ decays.

Process	Prediction 1	Prediction 2	Experiment
$\rho^+ \rightarrow \pi^+\gamma$	58	([†])	68 ± 7
$\rho^0 \rightarrow \pi^0\gamma$	58	68	120 ± 30
$\omega \rightarrow \pi^0\gamma$	452	546	717 ± 50
$\rho^0 \rightarrow \eta\gamma$	35	42	58 ± 11
$\omega \rightarrow \eta\gamma$	3	4	4 ± 2
$\phi \rightarrow \eta\gamma$	75(*)	91(*)	57 ± 3
$\eta' \rightarrow \rho^0\gamma$	41	50	59 ± 9
$\eta' \rightarrow \omega\gamma$	4	5	6 ± 1
$K^{*0} \rightarrow K^0\gamma$	110(*)	133(*)	116 ± 12
$K^{*+} \rightarrow K^+\gamma$	28(*)	34(*)	50 ± 6

([†]) Input to fix g_A ($g_A = 0.76$).

(*) These processes get contributions from explicit chiral symmetry breaking terms proportional to the strange-quark mass [22].

Instead, the most reliable prediction is for the $\rho^+ \rightarrow \pi^+\gamma$ decay because is not affected by neutral particle mixings and the explicit chiral symmetry breaking is small. All the other transitions are either affected by mixings or by sizable explicit

chiral symmetry breaking effects. The agreement between the result for the $\rho^+ \rightarrow \pi^+\gamma$ decay in the column Prediction 1 and experiment can be improved by using either a larger value for g_A or a smaller value for f_V (*i.e.* a larger value of x) or both. Given the poor knowledge of the parameter g_A and the rather good value for f_V we are using ($f_V = 0.17$ compared to the experimental value $f_V|_{\text{exp}} \simeq 0.20$), we shall fix the value of f_V to $f_V = 0.17$ and fix from the decay $\rho^+ \rightarrow \pi^+\gamma$ the value of g_A . We find then $g_A = 0.76$. So that, this value of g_A leads to $h_V = 0.033$. We shall use this value to see how the predictions in Table 2 vary with g_A . The corresponding results with $g_A = 0.76$ are in the column Prediction 2. We find that, in general, the results are improved, except for the decay $\phi \rightarrow \eta\gamma$ which is now 10 σ from the central experimental value. However, as was already stated, this decay rate is very sensitive to explicit chiral symmetry breaking. The prediction for the decay $\omega \rightarrow \pi^0\gamma$ improves but is still 3.5 σ from the experimental value which probably means that the $\omega_8 - \rho^0$ mixing is likely to be important.

Next, we shall study the predictions for the $V \rightarrow \pi\pi\pi$ decays for which the results can be found in Table 3. The Feynman diagrams for this process are shown in Figure 3. The amplitude for $\omega \rightarrow \pi^+\pi^-\pi^0$ has the form,

$$A(\omega \rightarrow \pi^+(p_1)\pi^-(p_2)\pi^0(p_3)) = \frac{6\sqrt{2}}{f_\pi^3} \theta_V \epsilon_{\mu\nu\alpha\beta} \varepsilon_{(\omega)}^{*\mu} p_1^\nu p_2^\alpha p_3^\beta \times \left[1 + \frac{4\sqrt{2}}{3} \frac{g_V \sigma_V}{\theta_V} \sum_{i,j=1,2,3}^{i<j} \frac{p_{ij}^2}{M_\rho^2 - p_{ij}^2 - i M_\rho \Gamma_\rho} \right] \quad (6.8)$$

with $p_{ij} = p_i + p_j$. The amplitudes for $\rho \rightarrow \pi\pi\pi$ decays vanish at lowest order. The decay rate for $\omega \rightarrow \pi^+\pi^-\pi^0$ is

$$\Gamma(\omega \rightarrow \pi^+\pi^-\pi^0) = \frac{1}{384 \pi^3 M_\omega} \int dE_+ \int dE_- \sum_{\text{pol}} |A|^2 \quad (6.9)$$

with $E_\pm \equiv E_{\pi^+} \pm E_{\pi^-}$. The limits in Eq. (6.9) are given by

$$(E_+)_{\text{max}} = M_\omega - m_\pi, \quad (E_+)_{\text{min}} = \frac{M_\omega}{2} + \frac{3m_\pi^2}{2M_\omega},$$

$$(E_-)_{\text{max}} = \frac{m_\pi^2 + M_\omega^2 - 2x - 2(M_{\pi^0\pi^-}^2)_{\text{min}}}{2M_\omega}, \quad (6.10)$$

$$(E_-)_{\text{min}} = \frac{m_\pi^2 + M_\omega^2 - 2x - 2(M_{\pi^0\pi^-}^2)_{\text{max}}}{2M_\omega},$$

with

$$\begin{aligned}
(M_{\pi^0\pi^-}^2)_{\min(\max)} &= \frac{1}{8(m_\pi^2 + x)} \left[(M_\omega^2 - m_\pi^2)^2 \right. \\
&\quad \left. - \left(\lambda^{1/2}(2(m_\pi^2 + x), m_\pi^2, m_\pi^2) + (-) \lambda^{1/2}(M_\omega^2, m_\pi^2, 2(m_\pi^2 + x)) \right) \right], \quad (6.11) \\
x \equiv p_1 \cdot p_2 &= M_\omega E_+ - \frac{M_\omega^2 + m_\pi^2}{2}.
\end{aligned}$$

Table 3: Partial widths in keV corresponding to $V \rightarrow \pi\pi\pi$, $V \rightarrow P_1 P_2 \gamma$, $V \rightarrow V' \gamma$ and $V \rightarrow V' \pi$ decays.

Process	Prediction 1	Prediction 2	Experiment
$\omega \rightarrow \pi^+ \pi^- \pi^0$	$6.8 \cdot 10^3$	$7.5 \cdot 10^3$	$(7.5 \pm 0.1) \cdot 10^3$
$\rho^0 \rightarrow \pi^+ \pi^- \pi^0$	0	0	< 20
$\rho^+ \rightarrow \pi^+ \pi^- \pi^+$	0	0	—
$\rho^+ \rightarrow \pi^+ \pi^0 \gamma$	31	29	—
$\rho^0 \rightarrow \pi^+ \pi^- \gamma$	4	7.5	(#)
$\rho^0 \rightarrow \pi^0 \pi^0 \gamma$	0.5	0.7	—
$\rho^0 \rightarrow \pi^0 \eta \gamma$	$2 \cdot 10^{-5}$	$3 \cdot 10^{-5}$	—
$\omega \rightarrow \pi^+ \pi^- \gamma$	0.16	0.23	< 30
$\omega \rightarrow \pi^0 \pi^0 \gamma$	0.08	0.12	< 3.4
$\omega \rightarrow \pi^0 \eta \gamma$	$5 \cdot 10^{-4}$	$7 \cdot 10^{-4}$	—
$\phi \rightarrow \overline{K}^0 K^0 \gamma$	$4 \cdot 10^{-9}$	$6 \cdot 10^{-9}$	—
$\omega \rightarrow \rho^0 \gamma$	0	0	—
$\phi \rightarrow \omega \gamma$	0	0	< 220
$\phi \rightarrow \rho^0 \gamma$	0	0	< 90
$\phi \rightarrow \omega \pi^0$	0	0	—

(#) This transition is dominated by bremsstrahlung off pions. In Ref. [28] an upper bound of 0.76 MeV is given for the structural bremsstrahlung.

The results in the column Prediction 1 in Table 3 are for the input values of g_A , M_Q and x in Eq. (6.2). Here, the experimental knowledge is very limited and there exist just upper bounds for several of the transitions. Only the decay rate for $\omega \rightarrow \pi^+ \pi^- \pi^0$ is known. In our model, this amplitude depends on the coupling constants θ_V and

σ_V . With the value of g_A from $\rho^+ \rightarrow \pi^+\gamma$ ($g_A = 0.76$), our predictions are those in the column Prediction 2 in Table 3.

We next proceed to the study of the $V \rightarrow P_1 P_2 \gamma$ decays. The predictions we get for them are also shown in Table 3 and the corresponding Feynman diagrams shown in Figure 4. We shall study first the decays with charged pseudoscalar mesons in the final state. The amplitude we obtain for the $\rho^0 \rightarrow \pi^+ \pi^- \gamma$ decay is

$$A(\rho^0 \rightarrow \pi^+(p_1)\pi^-(p_2)\gamma(k)) = 2\sqrt{2}|e|\frac{\alpha_V}{f_\pi^2}\varepsilon_{(\rho)}^{*\mu}\left(\varepsilon_\mu^{(\gamma)}k_\nu - \varepsilon_\nu^{(\gamma)}k_\mu\right)(p_1+p_2)^\nu; \quad (6.12)$$

for the $\rho^+ \rightarrow \pi^+\pi^0\gamma$ decay,

$$A(\rho^+ \rightarrow \pi^+(p_1)\pi^0(p_2)\gamma(k)) = 2\sqrt{2}|e|\frac{\alpha_V}{f_\pi^2}\varepsilon_{(\rho)}^{*\mu}\left(\varepsilon_\mu^{(\gamma)}k_\nu - \varepsilon_\nu^{(\gamma)}k_\mu\right) \times \left[p_2^\nu + \sqrt{2}\frac{g_V\phi_V}{\alpha_V}\frac{(p_1+p_2)^2(p_2-p_1)^\nu}{M_\rho^2 - (p_1+p_2)^2 - iM_\rho\Gamma_\rho} \right] \quad (6.13)$$

and for the $\omega \rightarrow \pi^+\pi^-\gamma$ decay,

$$A(\omega \rightarrow \pi^+(p_1)\pi^-(p_2)\gamma(k)) = -\frac{16\sqrt{2}}{3}|e|\frac{\sigma_V h_V}{f_\pi^2}\epsilon_{\mu\nu\alpha\beta}\epsilon_{.bcd}^{\beta}\varepsilon_{(\omega)}^{*\mu}\varepsilon_{(\gamma)}^c k^d \times \left(p_1^\nu(p_2+k)^\alpha p_2^b \frac{1}{M_\rho^2 - (p_2+k)^2 - iM_\rho\Gamma_\rho} + (p_1 \leftrightarrow p_2) \right). \quad (6.14)$$

The amplitudes corresponding to the decays $V^0 \rightarrow P^0 P^0 \gamma$ are

$$A(V^0 \rightarrow P^0(p_1)P^0(p_2)\gamma(k)) = -C_{VPP\gamma}16\sqrt{2}|e|\frac{\sigma_V h_V}{f_\pi^2}\epsilon_{\mu\nu\alpha\beta}\epsilon_{.bcd}^{\beta}\varepsilon_{(V)}^{*\mu}\varepsilon_{(\gamma)}^c k^d \times \left(p_1^\nu(p_2+k)^\alpha p_2^b \frac{1}{M_{V'}^2 - (p_2+k)^2 - iM_{V'}\Gamma_{V'}} + \left(\begin{array}{cc} p_1 & \leftrightarrow & p_2 \\ V' & \rightarrow & V'' \end{array} \right) \right). \quad (6.15)$$

The SU(3)-symmetry factors $C_{VPP\gamma}$ and the intermediate resonances V' and V'' are listed in Table 4.

The decay rate for all the $V \rightarrow P_1 P_2 \gamma$ decays can be written as follows

$$\Gamma(V \rightarrow P_1 P_2 \gamma) = \frac{1}{384\pi^3 M_V} \int dE_+ \int dE_- \sum_{\text{pol}} |A|^2 \quad (6.16)$$

Table 4: SU(3)-symmetry factors ($C_{VPP\gamma}$) and intermediate resonances (V', V'') for the $V^0 \rightarrow P^0 P^0 \gamma$ decays.

Process	$C_{VPP\gamma}$	V', V''
$\rho^0 \rightarrow \pi^0 \pi^0 \gamma$	1	ω, ω
$\omega \rightarrow \pi^0 \pi^0 \gamma$	1/3	ρ^0, ρ^0
$\rho^0 \rightarrow \pi^0 \eta \gamma$	$\sqrt{2}/(3\sqrt{3})$	ρ^0, ω
$\omega \rightarrow \pi^0 \eta \gamma$	$\sqrt{2}/\sqrt{3}$	ω, ρ^0
$\phi \rightarrow \pi^0 \pi^0 \gamma$	0	ρ^0, ρ^0
$\phi \rightarrow \pi^0 \eta \gamma$	0	ω, ρ^0
$\phi \rightarrow K^0 \overline{K^0} \gamma$	$-\sqrt{2}/3$	$K^{*0}, \overline{K^{*0}}$

with $E_{\pm} \equiv E_{P_1} \pm E_{P_2}$. The limits in Eq. (6.16) are given by

$$\begin{aligned}
(E_+)_{\max} &= M_V, & (E_+)_{\min} &= \frac{M_V}{2} + \frac{(m_{P_1} + m_{P_2})^2}{2M_V}, \\
(E_-)_{\max} &= \frac{m_{P_1}^2 - m_{P_2}^2 + M_V^2 - 2x - 2(M_{\gamma P_2}^2)_{\min}}{2M_V}, \\
(E_-)_{\min} &= \frac{m_{P_1}^2 - m_{P_2}^2 + M_V^2 - 2x - 2(M_{\gamma P_2}^2)_{\max}}{2M_V},
\end{aligned} \tag{6.17}$$

with

$$\begin{aligned}
(M_{\gamma P_2}^2)_{\min(\max)} &= \frac{1}{4(m_{P_1}^2 + m_{P_2}^2 + 2x)} \left[(M_V^2 + m_{P_2}^2 - m_{P_1}^2)^2 \right. \\
&\quad \left. - \left(\lambda^{1/2}(m_{P_1}^2 + m_{P_2}^2 + 2x, m_{P_1}^2, m_{P_2}^2) + (-) \lambda^{1/2}(M_V^2, 0, m_{P_1}^2 + m_{P_2}^2 + 2x) \right) \right], \\
x \equiv p_1 \cdot p_2 &= M_V E_+ - \frac{M_V^2 + m_{P_1}^2 + m_{P_2}^2}{2}.
\end{aligned} \tag{6.18}$$

For the transitions with two identical particles in the final state there is an additional factor 1/2 in the decay rate in Eq. (6.16). The amplitudes for the $\omega \rightarrow \rho^0 \gamma$, $\phi \rightarrow \omega \gamma$, $\phi \rightarrow \rho^0 \gamma$ and $\phi \rightarrow \omega \pi^0$ decays are zero at lowest order.

Up to now we have considered the $\omega - \phi$ mixing angle to be ideal. The $\phi \rightarrow \pi^0 \gamma$, $\phi \rightarrow \rho^+ \pi^-$, $\phi \rightarrow \pi^+ \pi^- \pi^0$ and $\phi \rightarrow P^0 P^0 \gamma$ decays are proportional to the deviation

of the actual $\omega - \phi$ mixing angle from the ideal one. The effect of a small deviation on the other ϕ vector decays studied before is not sizable. We define the deviation of the $\omega - \phi$ mixing angle from the ideal one as the difference

$$\epsilon \equiv \varphi_V - \varphi, \quad (6.19)$$

where φ is the physical $\omega - \phi$ mixing angle and φ_V is the ideal mixing angle. The amplitude for $\phi \rightarrow \rho^+ \pi^-$ we obtain is

$$A(\phi \rightarrow \rho^+(p_1)\pi^-(p_2)) = \epsilon \frac{8}{f_\pi} \sigma_V \epsilon_{\mu\nu\alpha\beta} \varepsilon_{(\phi)}^{*\mu} p_1^\nu \varepsilon_{(\rho)}^\alpha p_2^\beta, \quad (6.20)$$

giving the following decay rate

$$\Gamma = \epsilon^2 \frac{2}{3\pi} \sigma_V^2 \frac{M_\phi^3}{f_\pi^2} \lambda^{3/2} \left(1, \frac{M_\rho^2}{M_\phi^2}, \frac{m_\pi^2}{M_\phi^2} \right). \quad (6.21)$$

The amplitudes for the other transitions which are proportional to this deviation can be easily obtained by multiplying the corresponding transition amplitudes of the ω vector by a factor ϵ . The decay rates are the corresponding ones obtained by changing the ω vector parameters by the ϕ vector ones. We can predict this deviation if we assume that the measured partial widths in Ref. [6] for these transitions come only from a non-ideal mixing. First, we shall use the set of parameters in Eq. (6.2) for the input values of g_A , M_Q and x . From $\phi \rightarrow \pi^0 \gamma$ we then obtain the following result

$$\epsilon^2 = (5.7 \pm 0.8) \cdot 10^{-3}, \quad (6.22)$$

and from $\phi \rightarrow \rho^+ \pi^-$

$$\epsilon^2 = (7.6 \pm 0.5) \cdot 10^{-3}. \quad (6.23)$$

Using the average of these two results we predict the decay rates for the ϕ vector that are in the column Prediction 1 in Table 5.

If instead, we use the value of $g_A = 0.76$ found above from the decay $\rho^+ \rightarrow \pi^+ \gamma$ then, from $\phi \rightarrow \pi^0 \gamma$, we obtain

$$\epsilon^2 = (4.8 \pm 0.6) \cdot 10^{-3}, \quad (6.24)$$

and from $\phi \rightarrow \rho^+ \pi^-$

Table 5: Partial widths in keV corresponding to ϕ -decays assuming non-ideal $\omega - \phi$ mixing.

Process	Prediction 1	Prediction 2	Experiment
$\phi \rightarrow \pi^0 \gamma$	([†])	([†])	5.8 ± 0.8
$\phi \rightarrow \rho^+ \pi^-$	([†])	([†])	570 ± 40
$\phi \rightarrow \pi^+ \pi^- \gamma$	$6 \cdot 10^{-2}$	$7 \cdot 10^{-2}$	< 30
$\phi \rightarrow \pi^0 \pi^0 \gamma$	$3 \cdot 10^{-2}$	$4 \cdot 10^{-2}$	< 4.4
$\phi \rightarrow \pi^0 \eta \gamma$	$1.5 \cdot 10^{-2}$	$1.8 \cdot 10^{-2}$	< 11
$\phi \rightarrow \pi^+ \pi^- \pi^0$	65	60	106 ± 42

([†]) These data have been used as input.

$$\epsilon^2 = (6.3 \pm 0.5) \cdot 10^{-3}. \quad (6.25)$$

Using the average of these two new results we predict the decay rates for the ϕ vector that are in the column Prediction 2. The only decay rate that has been measured in Table 5 is 1 σ from our predictions.

6.2 The decay $\pi^0(\eta) \rightarrow \gamma \ell^+ \ell^-$

Here we shall study the process $\pi^0(\eta) \rightarrow \gamma \gamma^*$ (and the related one $e^+ e^- \rightarrow \omega, \rho^0 \rightarrow \pi^0 \gamma$) in the limit of complete vector dominance, *i.e.* assuming that the $\mathcal{O}(p^6)$ couplings are saturated by the contribution coming from integrating out the spin-1 particles as is the case for the $\mathcal{O}(p^4)$ chiral Lagrangian couplings [5]. The amplitudes for these processes acquire a dependence on the invariant mass of the off-shell photon from chiral $\mathcal{O}(p^6)$ terms. Thus, one can define a slope parameter as follows,

$$\rho \equiv \left(\frac{1}{A(P \rightarrow \gamma \gamma^*)} \frac{d}{ds^*} A(P \rightarrow \gamma \gamma^*) \right)_{s^*=0} \quad (6.26)$$

which is independent of the pseudoscalar meson P . The slope ρ has been measured in the $\pi^0 \rightarrow \gamma e^+ e^-$ transition [6] with the following result

$$\rho = (1.8 \pm 0.14) \text{ GeV}^{-2}. \quad (6.27)$$

It has been also measured in the $\eta \rightarrow \gamma e^+ e^-$ transition [6] and the result is

$$\rho = (1.4 \pm 0.2) \text{ GeV}^{-2}. \quad (6.28)$$

The weighted average from both results is

$$\rho = (1.68 \pm 0.2) \text{ GeV}^{-2}. \quad (6.29)$$

Theoretically, the slope ρ has two kinds of contributions. One from chiral loops (see Figure 5) and the other from the exchange of vector mesons (see Figure 6). The result we obtain in the ENJL model is the following

$$\rho = \frac{1}{\Lambda_l^2} + \frac{1}{M_V^2} \left(1 - \frac{2}{3} (1 - g_A) \right), \quad (6.30)$$

where $\Lambda_l^2 = 3.57 \text{ GeV}^2$ is the contribution from the chiral loops which has been estimated in Ref. [23]. The dependence in Eq. (6.30) on the coupling g_A comes from the combination of vector couplings $f_V h_V$. If we take for the parameters in Eq. (6.30) the ENJL predictions obtained with the choice in Eq. (6.2), *i.e.* $M_V = 0.8 \text{ GeV}$ and $g_A = 0.65$ [1], then we get

$$\rho = 1.48 \text{ GeV}^{-2}, \quad (6.31)$$

to be compared with the experimental result in Eq. (6.29). If instead, we take $g_A = 0.76$, which is the other value we have been using in the previous Section, we find

$$\rho = 1.59 \text{ GeV}^{-2}. \quad (6.32)$$

Both predictions are less than 1σ from the experimental result in Eq. (6.29).

Next, we want to study the related process $e^+e^- \rightarrow \omega, \rho^0 \rightarrow \pi^0\gamma$. The Feynman diagrams for this transition can be obtained from diagrams in Figure 5 and Figure 6 by inserting an e^+e^- pair in the off-shell photon leg. The cross section for this process is given by

$$\begin{aligned} \sigma_{e^+e^- \rightarrow \omega, \rho^0 \rightarrow \pi^0\gamma}(s) = & \frac{\alpha^3}{96 \pi^2 f_\pi^2} \left| \sum_{V=\omega, \rho^0} \left(C_l(\mu = M_V, s) + 1 \right. \right. \\ & \left. \left. + \left(1 - \frac{2}{3} (1 - g_A) \right) \frac{s}{M_V^2 - s - i\sqrt{s}\Gamma_V} \right) \right|^2 \end{aligned} \quad (6.33)$$

where we have used the full expression for the vector propagator as suggested in Ref. [24]. (In this Reference this cross section was given in the HGS model [15, 16].) The function $C_l(\mu, s)$ in Eq. (6.33) comes from chiral loops [24] and has the following expression

$$C_l(\mu, s) = \frac{1}{48\pi^2 f_\pi^2} \left[s \ln \frac{\mu^2}{m_\pi m_K} + \frac{5}{3} s + 2 F(m_\pi^2, s) + 2 F(m_K^2, s) \right]$$

with

$$F(m^2, s) = m^2 \left(1 - \frac{x}{4}\right) \left(1 - \frac{4}{x}\right)^{1/2} \ln \frac{\sqrt{x} + \sqrt{x-4}}{\sqrt{x} - \sqrt{x-4}} - 2m^2$$

for $x \equiv \frac{s}{m^2} > 4$ and

(6.34)

$$F(m^2, s) = m^2 \left(1 - \frac{x}{4}\right) \left(\frac{4}{x} - 1\right)^{1/2} \arctan \sqrt{\frac{x}{x-4}} - 2m^2$$

for $x \leq 4$.

The result we get for this cross section at the ω -mass peak using the set of parameters in Eq. (6.2) is

$$\sigma(e^+e^- \rightarrow \omega, \rho \rightarrow \pi^0\gamma)|_{s=M_\omega^2} = 94 \text{ nb},$$
(6.35)

to be compared with the experimental result [28],

$$\sigma(e^+e^- \rightarrow \omega, \rho \rightarrow \pi^0\gamma)|_{s=M_\omega^2} = (152 \pm 13) \text{ nb}.$$
(6.36)

If instead, we use the value for $g_A = 0.76$ we find

$$\sigma(e^+e^- \rightarrow \omega, \rho \rightarrow \pi^0\gamma)|_{s=M_\omega^2} = 113 \text{ nb}.$$
(6.37)

The last result is better (3 σ from the experimental result).

6.3 a_1 -decays

In this Section we shall study the decays corresponding to the axial-vector particle a_1 . These decays have been studied in Ref. [27] at the quark-loop level within a different ENJL model. The results we find for these decays are presented in Table 6

and the Feynman diagrams in Figure 7. This particle decays mainly into $\rho\pi$ and the full width reported in Ref. [6] ranges between 350 and 450 MeV. The amplitudes that we obtain for the transitions $a_1^+ \rightarrow \rho^+ \pi^0$ and $a_1^+ \rightarrow \rho^0 \pi^+$ are

$$\begin{aligned}
A(a_1^+ \rightarrow \rho^+(p_1)\pi^0(p_2)) &= -A(a_1^+ \rightarrow \rho^0(p_1)\pi^+(p_2)) \\
&= i \frac{2}{f_\pi} \left[A^{(2)} \left((p_1 + p_2)^\mu \varepsilon_{(a_1)}^{*\nu} - (p_1 + p_2)^\nu \varepsilon_{(a_1)}^{*\mu} \right) \varepsilon_\mu^{(\rho)} p_{2,\nu} \right. \\
&\quad \left. + A^{(3)} \left(p_1^\mu \varepsilon_{(\rho)}^\nu - p_1^\nu \varepsilon_{(\rho)}^\mu \right) \varepsilon_\mu^{*(a_1)} p_{2,\nu} \right]
\end{aligned} \tag{6.38}$$

with the following corresponding decay rates

$$\Gamma(a_1^+ \rightarrow \rho\pi) = \frac{1}{48 \pi M_{a_1}} \lambda^{1/2} \left(1, \frac{m_\rho^2}{M_{a_1}^2}, \frac{M_\rho^2}{M_{a_1}^2} \right) \sum_{\text{pol}} |A|^2. \tag{6.39}$$

We have also studied the direct decays into three pions of the a_1 axial-vector. The amplitude we get for the transition $a_1^+ \rightarrow \pi^+ \pi^0 \pi^0$ is the following

$$\begin{aligned}
A(a_1^+ \rightarrow \pi^+(p_1)\pi^0(p_2)\pi^0(p_3)) &= -i \frac{2\sqrt{2}}{f_\pi^3} \varepsilon_{(a_1)}^{*\mu} \left[(\gamma^{(1)} + \gamma^{(3)}) \right. \\
&\quad \left. \times ((p_1 \cdot p_2) p_{3,\mu} + (p_1 \cdot p_3) p_{2,\mu}) + (2\gamma^{(2)} - \gamma^{(1)} + 2\gamma^{(4)}) (p_2 \cdot p_3) p_{1,\mu} \right];
\end{aligned} \tag{6.40}$$

and for $a_1^+ \rightarrow \pi^- \pi^+ \pi^+$,

$$\begin{aligned}
A(a_1^+ \rightarrow \pi^-(p_1)\pi^+(p_2)\pi^+(p_3)) &= -i \frac{2\sqrt{2}}{f_\pi^3} \varepsilon_{(a_1)}^{*\mu} \left[2 (\gamma^{(1)} + \gamma^{(3)}) (p_2 \cdot p_3) p_{1,\mu} \right. \\
&\quad \left. + (2\gamma^{(2)} + \gamma^{(3)} + 2\gamma^{(4)}) ((p_1 \cdot p_2) p_{3,\mu} + (p_1 \cdot p_3) p_{2,\mu}) \right].
\end{aligned} \tag{6.41}$$

The experimental information we have is just on $a_1 \rightarrow (\pi\pi)_S \pi$ decays, *i.e.* where two of the pions are in an S-wave. For this process there is an educated guess in Ref. [6] (the error is of the same order) for the experimental upper bound which is around 3 MeV. If we assume that the reported partial width for the decay $a_1 \rightarrow (\pi\pi)_S \pi$ is only due to direct production and not to a possible intermediate scalar particle, *i.e.*

$a_1 \rightarrow a_0(f_0)\pi \rightarrow (\pi\pi)_S \pi$ that would have been eventually detected, then we obtain the following amplitudes. For the transition $a_1^+ \rightarrow (\pi^+\pi^0)_S \pi^0$,

$$A(a_1^+ \rightarrow (\pi^+(p_1)\pi^0(p_2))_S \pi^0(p_3)) = -i \frac{2\sqrt{2}}{f_\pi^3} (\gamma^{(1)} + \gamma^{(3)}) (\varepsilon_{(a_1)}^* \cdot p_3) (p_1 \cdot p_2); \quad (6.42)$$

and for the $a_1^+ \rightarrow (\pi^-\pi^+)_S \pi^+$,

$$A(a_1^+ \rightarrow (\pi^-(p_1)\pi^+(p_2))_S \pi^+(p_3)) = -i \frac{2\sqrt{2}}{f_\pi^3} (2\gamma^{(2)} + \gamma^{(3)} + 2\gamma^{(4)}) (\varepsilon_{(a_1)}^* \cdot p_3) (p_1 \cdot p_2). \quad (6.43)$$

The decay rate for $a_1^+ \rightarrow \pi^-\pi^+\pi^+$ (for $a_1^+ \rightarrow \pi^+\pi^0\pi^0$ and $a_1^+ \rightarrow (\pi\pi)_S \pi$ are analogous) can be written as follows

$$\Gamma(a_1^+ \rightarrow \pi^-\pi^+\pi^+) = \frac{1}{768 \pi^3 M_{a_1}} \int dE_+ \int dE_- \sum_{\text{pol}} |A|^2 \quad (6.44)$$

with $E_\pm = E_{\pi^+} \pm E_{\pi^-}$ and the limits given by

$$\begin{aligned} (E_+)_{\max} &= M_{a_1} - m_\pi, & (E_+)_{\min} &= \frac{M_{a_1}}{2} + \frac{3m_\pi^2}{2M_{a_1}}, \\ (E_-)_{\max} &= \frac{m_\pi^2 + M_{a_1}^2 - 2x - 2(M_{\pi^+\pi^-}^2)_{\min}}{2M_{a_1}}, \\ (E_-)_{\min} &= \frac{m_\pi^2 + M_{a_1}^2 - 2x - 2(M_{\pi^+\pi^-}^2)_{\max}}{2M_{a_1}}, \end{aligned} \quad (6.45)$$

with

$$\begin{aligned} (M_{\pi^+\pi^-}^2)_{\min(\max)} &= \frac{1}{8(m_\pi^2 + x)} \left[(M_{a_1}^2 - m_\pi^2)^2 \right. \\ &\quad \left. - \left(\lambda^{1/2}(2(m_\pi^2 + x), m_\pi^2, m_\pi^2) + (-) \lambda^{1/2}(M_{a_1}^2, m_\pi^2, 2(m_\pi^2 + x)) \right) \right], \end{aligned} \quad (6.46)$$

$$x \equiv p_1 \cdot p_2 = M_{a_1} E_+ - \frac{M_{a_1}^2 + m_\pi^2}{2}.$$

Another interesting decay is $a_1^+ \rightarrow \rho^+ \gamma$. The amplitude we obtain is

$$A(a_1^+ \rightarrow \rho^+(p)\gamma(k)) = i|e|\frac{4}{3}H\epsilon_{\mu\nu\alpha\beta}\epsilon_{(\rho)}^\mu\epsilon_{(a_1)}^{*\nu}k^\alpha\epsilon_{(\gamma)}^\beta \quad (6.47)$$

and the corresponding decay rate

$$\Gamma(a_1^+ \rightarrow \rho^+\gamma) = \alpha\frac{2}{27}H^2M_{a_1}\left(1 - \frac{M_\rho^2}{M_{a_1}^2}\right)^3\left(1 + \frac{M_\rho^2}{M_{a_1}^2}\right). \quad (6.48)$$

Finally, we shall report on the decay $a_1^+ \rightarrow \pi^+\gamma$. The amplitude we get for this process is

$$A(a_1^+ \rightarrow \pi^+(p)\gamma(k)) = -i|e|\frac{f_A - 2\sqrt{2}\alpha_A}{2f_\pi} \\ \times (\epsilon_{(a_1)}^{*\mu}(p+k)^\nu - \epsilon_{(a_1)}^{*\nu}(p+k)^\mu)(\epsilon_\mu^{(\gamma)}k_\nu - \epsilon_\nu^{(\gamma)}k_\mu) \quad (6.49)$$

and the corresponding decay rate

$$\Gamma(a_1^+ \rightarrow \pi^+\gamma) = \alpha\frac{M_{a_1}^3}{24f_\pi^2}(f_A - 2\sqrt{2}\alpha_A)^2\left(1 - \frac{m_\pi^2}{M_{a_1}^2}\right)^3. \quad (6.50)$$

The predictions for all these decays for the set of input parameters in Eq. (6.2) are the ones in the column Prediction 1 in Table 6.

The result we obtain for the full width of the a_1 axial-vector from the results in the column Prediction 1 is $\Gamma_{\text{full}} = 261$ MeV, to be compared with the experimental value quoted at the beginning of this Section ($350 \text{ MeV} < (\Gamma_{\text{full}})_{\text{exp}} < 450 \text{ MeV}$).

In the column Prediction 2 we present the results obtained using the value $g_A = 0.76$. Given the poor experimental information we have on a_1 -decays, both sets of predictions in Table 6 are quite good. However, the full width for the a_1 axial-vector particle we obtain from the results in the column Prediction 2, $\Gamma_{\text{full}} = 359$ MeV, is better when compared with the experimental result quoted above.

6.4 $K_L \rightarrow \pi^0\gamma^*\gamma^* \rightarrow \pi^0e^+e^-$

The decay $K_L \rightarrow \pi^0e^+e^-$ has received a great deal of attention as a possible candidate for observing CP-violation effects (for a review see Ref. [29]). The K_L

Table 6: Partial widths in MeV corresponding to the a_1 -decays.

Process	Prediction 1	Prediction 2	Experiment
$a_1^+ \rightarrow \rho^+ \pi^0$	130	178	dominant
$a_1^+ \rightarrow \rho^0 \pi^+$	129	176	dominant
$a_1^+ \rightarrow \pi^+ \pi^0 \pi^0$	0.8	1.9	—
$a_1^+ \rightarrow \pi^- \pi^+ \pi^+$	1.0	2.5	—
$a_1^+ \rightarrow (\pi\pi)_S \pi$	0.6	1.4	< 3 (*)
$a_1^+ \rightarrow \rho^+ \gamma$	$5 \cdot 10^{-3}$	$5 \cdot 10^{-3}$	—
$a_1^+ \rightarrow \pi^+ \gamma$	0.52	0.71	0.64 ± 0.25

(*) This is an educated guess, the experimental error is of the same order [6].

state consists mostly of a CP-odd state K_2 with a small mixing of the CP-even state K_1 ,

$$K_L \simeq K_2 + \epsilon K_1 \quad (6.51)$$

where $|\epsilon| \simeq 2.26 \times 10^{-3}$ is the standard CP-violation parameter in $K \rightarrow \pi\pi$ decays. This decay is interesting because “direct” CP-violation in the K_2 -decay amplitude and “indirect” (ϵ effect) CP-violation branching ratios are estimated to be of the same order [30]-[34]. (Of the order of 10^{-11} [33, 34].)

In addition to these CP-violating decay modes there is a two-photon exchange contribution to the transition $K_L \rightarrow \pi^0 e^+ e^-$ which is CP-conserving. In order to interpret future experimental measurements of this decay it is crucial to elucidate if this decay mode may compete or not with the CP-violating one-photon exchange contributions. The two-photon exchange decay mode was studied in Ref. [30] at $\mathcal{O}(p^4)$ in the context of chiral perturbation theory and was shown to be suppressed at this order [30, 31]. At $\mathcal{O}(p^6)$ there is a vector meson exchange diagram (shown in Figure 8) for the CP-conserving two-photon exchange contribution which a priori could be potentially large [35] and may compete with the one-photon CP-violating decay modes. We can make a prediction for the absorptive $\mathcal{O}(p^6)$ vector meson dominance (VMD) contribution to the process $K_L \rightarrow \pi^0 \gamma^* \gamma^* \rightarrow \pi^0 e^+ e^-$ in the model we are considering. To this VMD prediction one must add further direct weak $\mathcal{O}(p^6)$ contributions, as was pointed out in Ref. [36]. In this Reference, the whole $\mathcal{O}(p^6)$ contribution to $K_L \rightarrow \pi^0 \gamma^* \gamma^* \rightarrow \pi^0 e^+ e^-$ was estimated by using the so-called “weak deformation” model. Disregarding the $\mathcal{O}(p^4)$ helicity suppressed

contributions, these authors find

$$\text{BR} (K_2 \rightarrow \pi^0 e^+ e^-) |_{\text{Abs}} \simeq 4.4 a_V^2 10^{-12} \quad (6.52)$$

with

$$|a_V| \equiv \frac{512 \pi^2 h_V^2 m_{K^0}^2}{9 M_V^2} \quad (6.53)$$

where h_V is the vector coupling introduced in the Lagrangian in Eq. (2.9) and the intermediate resonance V denotes the ρ^0 and ω vector particles.

With our determination of this coupling and using the set of input parameters in Eq. (6.2), we obtain $h_V = 0.030$ which leads to

$$|a_V| = 0.21. \quad (6.54)$$

If we use the higher value for $g_A = 0.76$, which as we have seen is favoured by the overall data on spin-1 particle decays, then we obtain $h_V = 0.033$ which leads to

$$|a_V| = 0.25. \quad (6.55)$$

These values for $|a_V|$ are in good agreement with the different phenomenological estimates [34, 36] made for the branching ratio in Eq. (6.52).

Recently, a measurement of the branching ratio for the CP-conserving decay $K_L \rightarrow \pi^0 \gamma \gamma$ has been reported by the NA31 experiment at CERN [37]. This measurement gives the following bounds at 90 % C.L.,

$$-0.32 < a_V < 0.19. \quad (6.56)$$

7 Conclusions

In this work we have studied in the context of the ENJL cut-off model considered in Ref. [1] the anomalous and non-anomalous sectors of the chiral Lagrangian for spin-1 particles to $\mathcal{O}(p^3)$, including terms with two spin-1 particles. In this model, spin-1 particles are introduced not as gauge fields, in contrast to models in Refs. [15]-[18], but as fields which transform homogeneously. This feature gives rise to a formal symmetry of the QCD effective action (see Section 3), first noticed in Ref. [1], that we use extensively throughout the text. We have calculated 8 couplings in the

anomalous sector and 28 in the non-anomalous sector, both for terms involving spin-1 particles. In particular, we have given the dependence of these anomalous and non-anomalous couplings on the axial-coupling g_A . In this ENJL model, all the couplings we have calculated here and those in the strong chiral Lagrangian describing the interactions between Goldstone bosons [1] can be determined as functions of just three parameters, namely g_A , defined in Eqs. (3.15) and (6.1), $x \equiv M_Q^2/\Lambda_\chi^2$ and M_Q . Taking the values for these three parameters that fit the chiral $\mathcal{O}(p^2)$ and $\mathcal{O}(p^4)$ low-energy couplings (see Ref. [1]) we have given predictions for the following low-energy processes: $V \rightarrow \pi\gamma$, $V \rightarrow \pi\pi\pi$, $V \rightarrow \pi\pi\gamma$, $V \rightarrow V'\gamma$, $V \rightarrow V'\pi$, $A \rightarrow \pi\pi\pi$, $A \rightarrow \pi\gamma$, $A \rightarrow V\pi$ and $A \rightarrow V\gamma$ at low orders in the chiral expansion. The vector meson dominance limit predictions for $\pi^0 \rightarrow \gamma\gamma^*$ and $K_L \rightarrow \pi^0\gamma^*\gamma^* \rightarrow \pi^0 e^+e^-$ processes have also been discussed. The results are, in general, in good agreement with the present experimental data taking into account that they have been obtained in the chiral limit. In addition, we make predictions for decay rates which can be measured in future low-energy experiments. We have also seen that the available overall data on spin-1 decays prefer a slightly higher value for the axial coupling g_A than the one reported in Ref. [1] obtained from a fit to the low-energy data to chiral $\mathcal{O}(p^4)$. In conclusion, we find that the ENJL model we have been considering reproduces quite well a large variety of low-energy processes where spin-1 particles are involved and the predictions we make depend on just a small number of parameters (three) which can be fixed from other low-energy transitions.

Acknowledgements

It is a pleasure to thank Eduardo de Rafael for continuous encouragement and very helpful discussions. I also wish to thank Hans Bijnens and Toni Pich for useful conversations and Lars Hörnfeldt for his help with the algebraic manipulation program STENSOR. This work has been supported in part by CICYT, Spain, under Grant No. AEN90-0040. I am indebted to the Spanish Ministerio de Educación y Ciencia for a fellowship.

References

- [1] J. Bijnens, C. Bruno and E. de Rafael, Nambu–Jona-Lasinio-Like Models and the Low Energy Effective Action of QCD, CERN and Marseille preprint CERN-TH.6521/92, CPT-92/P.2710 (1992), to appear in Nucl. Phys. **B**
- [2] S. Weinberg, Physica **A96** (1979) 327

- [3] J. Gasser and H. Leutwyler, *Ann. of Phys.* **158** (1984) 142; *Nucl. Phys.* **B250** (1985) 465, 517, 539
- [4] D. Espriu, E. de Rafael and J. Taron, *Nucl. Phys.* **B345** (1990) 22; (Erratum: *ibid.* **B355** (1991) 278)
- [5] G. Ecker, J. Gasser, A. Pich and E. de Rafael, *Nucl. Phys.* **B321** (1989) 311
- [6] Particle Data Group, K. Hikasa et al., *Phys. Rev.* **D45**, Part II (1992) S1
- [7] S. Coleman, J. Wess and B. Zumino, *Phys. Rev.* **177** (1969) 2237;
C.G. Callan, S. Coleman, J. Wess and B. Zumino, *Phys. Rev.* **177** (1969) 2247
- [8] G. Ecker, J. Gasser, H. Leutwyler, A. Pich and E. de Rafael, *Phys. Lett.* **B223** (1989) 425
- [9] A. Manohar and H. Georgi, *Nucl. Phys.* **B234** (1984) 189
- [10] J. Bijnens, *Nucl. Phys.* **B367** (1991) 709
- [11] J. Wess and B. Zumino, *Phys. Lett.* **37B** (1971) 95
- [12] E. Witten, *Nucl. Phys.* **B223** (1983) 422
- [13] W.A. Bardeen and B. Zumino, *Nucl. Phys.* **B244** (1984) 421
- [14] H. Leutwyler, *Phys. Lett.* **B152** (1985) 78
- [15] M. Bando, T. Kugo and K. Yamawaki, *Phys. Rep.* **164** (1988) 217; and References therein
- [16] T. Fujiwara, T. Kugo, H. Terao, S. Uehara and K. Yamawaki, *Prog. Theor. Phys.* **73** (1985) 926
- [17] Ö. Kaymakçalan, S. Rajeev and J. Schechter, *Phys. Rev.* **D30** (1984) 594;
H. Gomm, Ö. Kaymakçalan and J. Schechter, *Phys. Rev.* **D30** (1984) 2345;
Ö. Kaymakçalan and J. Schechter, *Phys. Rev.* **D31** (1985) 1109
- [18] U.-G. Meissner, *Phys. Rep.* **161** (1988) 213
- [19] M. Wakamatsu, *Ann. of Phys.* **193** (1989) 287
- [20] R.D. Ball, *Phys. Rep.* **182** (1989) 1; and References therein
- [21] J. Gasser and H. Leutwyler, *Phys. Rep.* **87** (1982) 77

- [22] R.S. Chivukula and J.M. Flynn, Phys. Lett. **168B** (1986) 127
- [23] J. Bijnens, A. Bramon and F. Cornet, Z. Phys. **C46** (1990) 599
- [24] A. Bramon, A. Grau and G. Pancheri, Phys. Lett. **B277** (1992) 353 ;
E. Pallante and R. Petronzio, Anomalous Effective Lagrangians and Vector Resonance Models, Roma preprint ROM2F 92/04 (1992)
- [25] A. Bramon, A. Grau and G. Pancheri, Phys. Lett. **B283** (1992) 416 ;
S. Fajfer and R.J. Oakes, Phys. Rev. **D42** (1990) 2392 ;
N.N. Achasov and V.N. Ivanchenko, Nucl. Phys. **B315** (1989) 465 ;
F.M. Renard, Nuovo Cim. **62A** (1969) 475
- [26] The DAΦNE Physics Handbook, INFN - LNF, Frascati, eds. L. Maiani, G. Pancheri and N. Paver (1992)
- [27] A.N. Ivanov, M. Nagy and N.I. Troitskaya, Int. J. of Mod. Phys. **A7** (1992) 7305; Phys. Lett. **B200** (1988) 171
- [28] S.I. Dolinsky et al., Phys. Rep. **202** (1991) 99
- [29] A. Pich, Nucl. Phys. B (Proc. Suppl.) **23B** (1991) 399; and References therein
- [30] G. Ecker, A. Pich and E. de Rafael, Nucl. Phys. **B291** (1987) 692
- [31] J.F. Donoghue, B.R. Holstein and G. Valencia, Phys. Rev. **D35** (1987) 2769
- [32] G. Ecker, A. Pich and E. de Rafael, Nucl. Phys. **B303** (1988) 665
- [33] C.O. Dib, I. Dunietz and F.J. Gilman, Phys. Lett. **B218** (1989) 487 ; Phys. Rev. **D39** (1989) 2639
- [34] J.M. Flynn and L. Randall, Nucl. Phys. **B326** (1989) 31
- [35] L.M. Sehgal, Phys. Rev. **D38** (1988) 808 ; *ibid.* **D41** (1990) 161 ;
T. Morozumi and H. Iwasaki, Prog. Theor. Phys. **82** (1989) 371 ;
J.M. Flynn and L. Randall, Phys. Lett. **B216** (1989) 221 ;
P. Ko, Phys. Rev. **D44** (1991) 139
- [36] G. Ecker, A. Pich and E. de Rafael, Phys. Lett. **B237** (1990) 481
- [37] G.D. Barr et al., Phys. Lett. **B284** (1992) 440

FIGURE CAPTIONS

Figure 1: Diagrams contributing to the process $V \rightarrow P\gamma$ ($P \rightarrow V\gamma$).

Figure 2: Pion and kaon chiral loops contribution to the process $\rho \rightarrow \pi\gamma$.

Figure 3: Diagrams contributing to the process $V \rightarrow \pi\pi\pi$.

Figure 4: Diagrams contributing to the process $V \rightarrow P_1P_2\gamma$.

Figure 5: Pion and kaon chiral loops contribution to the process $P^0 \rightarrow \gamma\gamma^*$.

Figure 6: Vector-exchange contribution to the process $P^0 \rightarrow \gamma\gamma^*$.

Figure 7: Diagrams for the a_1 -decays.

Figure 8: Vector-exchange contribution to the $K_L \rightarrow \pi^0\gamma^*\gamma^* \rightarrow \pi^0e^+e^-$ transition.

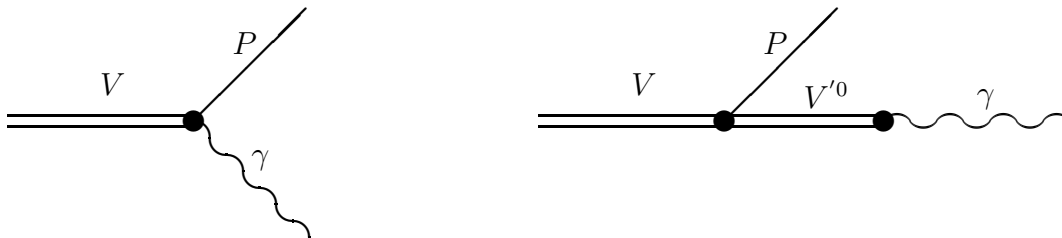


Figure 1:

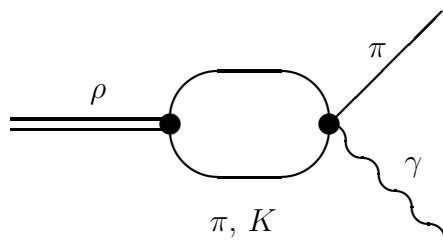


Figure 2:

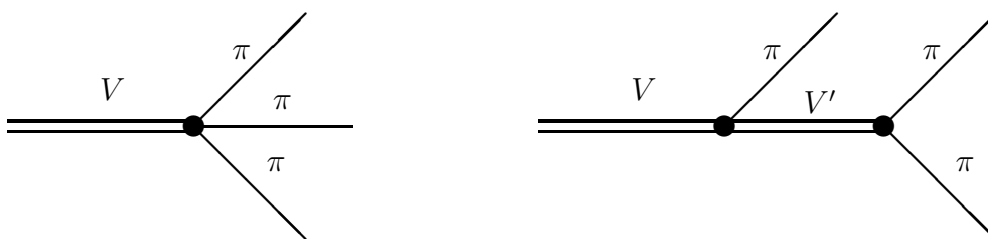


Figure 3:

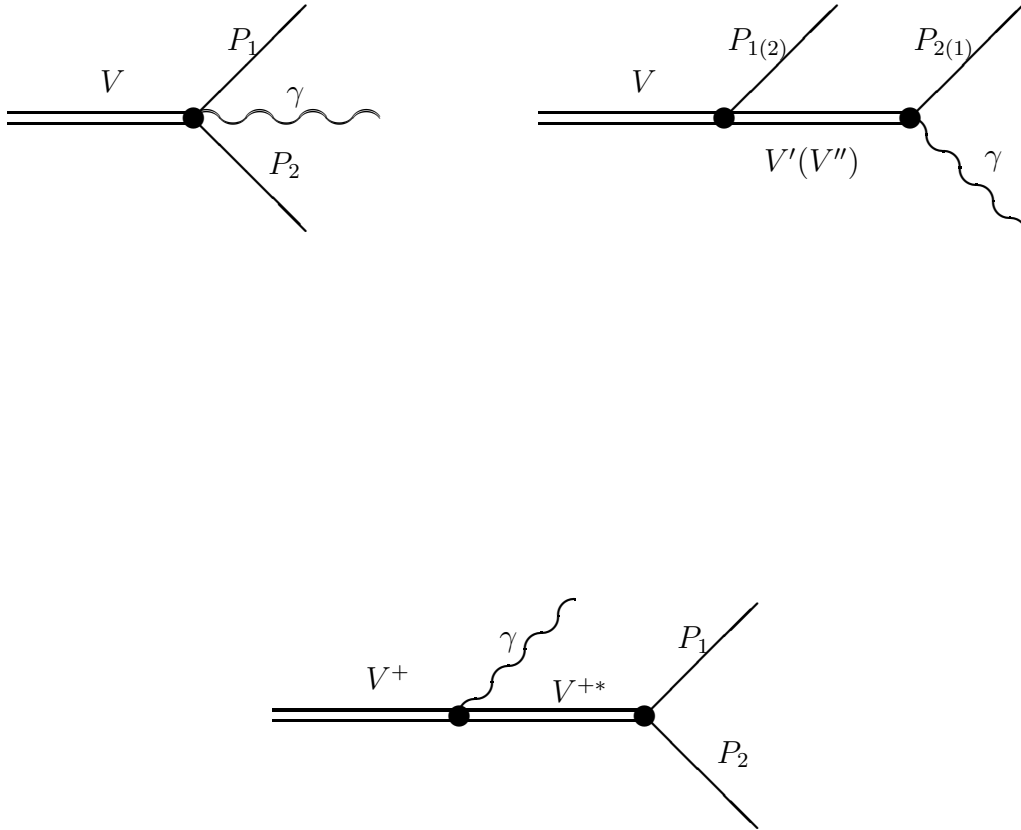


Figure 4:

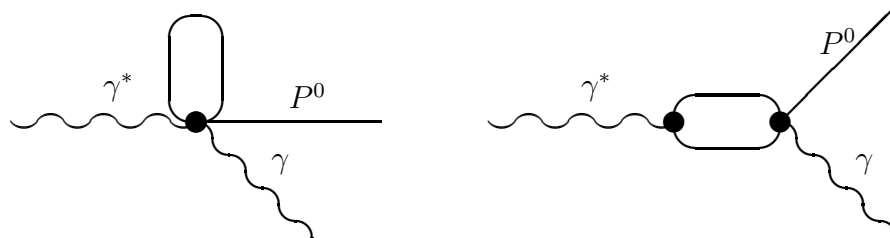


Figure 5:

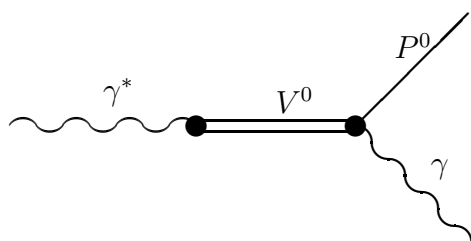


Figure 6:

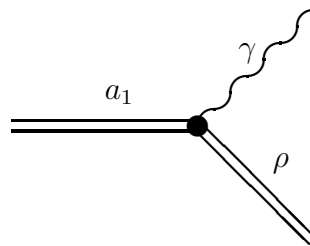
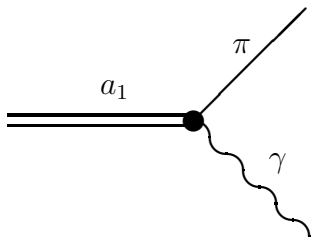
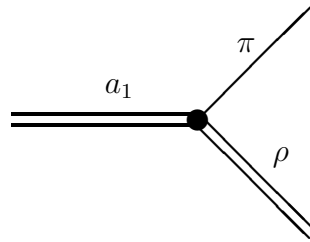
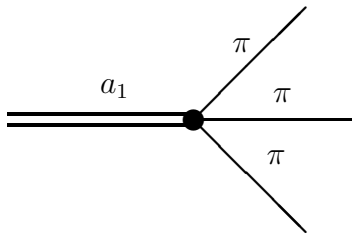


Figure 7:

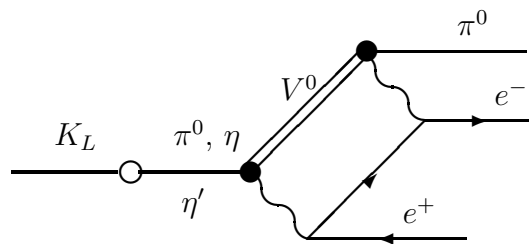


Figure 8: